



Advanced Bioimaging Technologies Conference Program - 2011

**September 7-9, 2011
Kraków, Poland**

Organised by:

H. Niewodniczański Institute of Nuclear Physics Polish Academy of Sciences
Institute for Biodiagnostics National Research Council of Canada
AGH University of Science and Technology

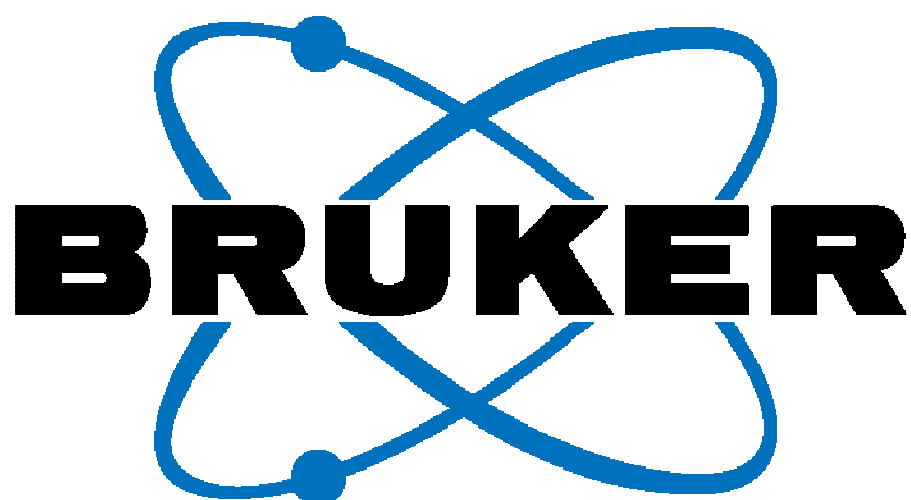
Kindly supported by:

Polish Academy of Sciences

Bruker

Siemens

Venue: AGH University of Science and Technology
Al. Mickiewicza, Kraków
Building C1, Room 224



SIEMENS

Conference Agenda

Tuesday, September 6

Registration	
15:00 - 18:00	Registration, Polonez Hotel

Wednesday, September 7

Registration	
8:00 - 12:00	Registration, AGH, Building C1

Welcome	
9:00 - 9:15	<i>Welcome Remarks</i>

1. Brain MRI 1 – Chair: Dr Władysław Węglarz, Institute of Nuclear Physics Polish Academy of Sciences, Kraków	
9:15 - 9:35	Stefan Wolfsberger, University of Vienna, Austria <i>Application of High Field MRI for Neurosurgery</i>
9:35 - 9:55	Aygül Mert, University of Vienna, Austria <i>Evaluation of High-quality 3D Brain Surface Visualization for Brain Tumor Surgery</i>
9:55 - 10:15	Andre Obenaus, Loma Linda University, Loma Linda, California, USA <i>Neuroimaging the Sequelae of Mild Traumatic Brain Injury</i>
10:15 - 10:35	Krzysztof Turek, AGH University of Science and Technology, Kraków, Poland <i>How about MRI in Space?</i>

10:35 - 11:15	Coffee Break
---------------	--------------

2. Grand Opening of 0.2T MRI at AGH	
11:15 - 12:30	Daniel Costello, Canadian Ambassador to Poland Antoni Tajduś, AGH University of Science and Technology, Kraków, Poland Wojciech Łużny, AGH University of Science and Technology, Kraków, Poland Henryk Figiel, AGH University of Science and Technology, Kraków, Poland

12:30 - 13:30	Lunch
---------------	-------

3. Molecular Imaging 1 – Chair: Dr. Uwe Himmelreich, Katholieke Universteit Leuven, Belgium	
13:30 - 13:50	Abedelnasser Abulrob, National Research Council, Ottawa, Canada <i>Molecular Imaging: Nanobodies meet Nanoparticles</i>
13:50 - 14:10	Luca Menichetti, CNR Istituto di Fisiologia Clinica, Pisa, Italy <i>In Vivo Imaging of Integrin Over-expression in Rat Myocardial Infarction</i>
14:10 - 14:30	Danica Stanimirovic, National Resarch Council, Ottawa, Canada <i>Bioimaging Modalities in Discovery and Validation of Biomarkers for Brain Diseases</i>
14:30 - 15:30	Coffee Break
4. Molecular Imaging 2 – Chair: Dr. Roxanne Deslauriers, Institute for Biodiagnostics, Canada	
15:30 - 15:50	Jens-Christoph Georgi, Siemens AG, Erlangen, Germany <i>Molecular MRI: a New Modality on its way into Clinical Routine</i>
15:50 -16:10	Uwe Himmelreich, Katholieke Universteit Leuven, Leuven, Belgium <i>What Contributions can MRI make for Non-invasive Cell Tracking?</i>
16:10 -16:30	Ganghong Tian, National Research Council, Winnipeg, Canada <i>Adipose Tissue is a Potential Source of Multipotent Stem Cells for Treatment of Heart Failure</i>
16:30 - 18:00	Poster Session

Thursday, September 8

9:15	9:45	Transfer from AGH to IFJ/PAN (meeting point: hotel Polonez, parking lot)
5. Tribute to Andrzej Jasinski: Auditorium IFJ PAN		
10:00	10:45	
6. Grand Opening of 9.4T MRI at IFJ PAN		
11:00	12:00	Marek Jeżabek, Institute of Nuclear Physics, Kraków, Poland Stefan Chłopicki, Jagiellonian Centre for Experimental Therapeutics, Kraków, Poland Andrew Lonergan, Bruker UK Limited, Coventry, UK Władysław Węglarz, Institute of Nuclear Physics, Kraków, Poland
12:00	12:30	Transfer from IFJ to AGH (meeting point: Main Building, front entrance)
12:30	- 13:30	Lunch
7. Hyperpolarization and New Imaging Techniques – Chair: Prof. Tomasz Dohnalik, Institute of Physics, Jagiellonian University, Kraków		
13:30	13:50	Jonathan Sharp, National Research Council, Calgary, Canada <i>Progress in Imaging with the RF Phase Gradient: The TRASE Method</i>
13:50	- 14:10	Jan-Bernd Hövener, University Hospital Freiburg, Freiburg, Germany <i>Beyond Boltzmann: Hyperpolarized Color MRI</i>
14:10	- 14:30	Paweł Grieb, Mossakowski Medical Research Centre, Warsaw, Poland <i>Methods of Hyperpolarization</i>
14:30	-14:50	Tadeusz Pałasz, Jagiellonian University, Kraków, Poland <i>MEOP Polarisation of ³He for Clinical Lungs Imaging</i>
14:50	- 15:20	Coffee Break
8. MR Applications – Closer to Clinic – Chair: Andre Obenaus, Loma Linda University, Loma Linda, USA		
15:20	- 15:40	Ian C.P. Smith, National Research Council, Winnipeg, Canada <i>Clinically Accurate Cancer Diagnosis by MR Spectroscopy</i>
15:40	- 16:00	Ray Somorjai, National Research Council, Winnipeg, Canada <i>Classification-based Accurate and Robust Diagnoses of Complex: An Essential Step Towards Clinical Use</i>
16:00	- 16:20	Daniel Muruve, University of Calgary, Calgary, Canada <i>Inflammation and Disease: Opportunities for Imaging</i>
16:20	-16:40	Piotr Kulinowski, Institute of Nuclear Physics, Krakow, Poland <i>Study of the Evolution of HPMC Based Matrix Systems During Hydration using 1H MRI</i>
18:00	- 22:00	Dinner

Friday, September 9

9. Brain Imaging and Image-Guided Surgery – Chair: Prof. Paweł Grieb, IMDiK, Warsaw, Poland	
9:00 - 9:25	Harald Möeller, Max Planck Institute for Human Cognitive and Brain Sciences, Leipzig, Germany <i>Orientation Dependence in Magnetization-transfer Imaging of Human White Matter</i>
9:25 - 9:55	Garnette Sutherland, University of Calgary, Calgary, Canada <i>Image-guided Robotics in Neurosurgery</i>
9:55 - 10:20	Mihaela Onu, Prof. Dr. T. Burghel Hospital, Bucharest, Romania <i>Diffusion MR Techniques in Tissue Microstructure Investigation</i>
10:20 - 11:30	Coffee Break
10. High Field MRI - Chair: Dr. Jonathan Sharp, IBD, Calgary, Canada	
11:30 - 11:50	Franz Schmitt, Siemens AG, MED MREF, Erlangen, Germany <i>UHF Imaging Updates</i>
11:50 - 12:10	Scott King, National Research Council, Winnipeg, Canada <i>MRI RF Coil Design for better SNR, Speed and Excitation</i>
12:10 - 12:30	Piotr Kozłowski, The Prostate Centre in Vancouver, Vancouver, Canada <i>Characterizing White Matter in Rat Spinal Cord with Quantitative MRI</i>
12:30 - 13:30	Lunch
11. New Imaging Techniques and Technologies - Chair: Dr. Franz Schmitt, Siemens, Germany	
13:30 - 13:50	Karol Jackowski, Warsaw University, Warszawa, Poland <i>Intermolecular Effects in ^3He and ^{129}Xe NMR Spectra</i>
13:50 - 14:10	Franciszek Hennel, Bruker Medical, Ettlingen, Germany <i>MRI with Ultrashort (and Zero) Echo Time</i>
14:10 - 14:30	Martin Uecker, am Max-Planck-Institut für biophysikalische Chemie, Göttingen, Germany <i>Real-time Magnetic Resonance Imaging at High Temporal Resolution</i>
14:30 - 14:50	Krzysztof Jasiński, Institute of Nuclear Physics, Krakow, Poland <i>RF Coils for Microimaging</i>
12. Closing	
14:50	Closing Remarks

Abstracts of Oral Presentations

Application of High Field MRI for Neurosurgery

Stefan Wolfsberger

Department of Neurosurgery, Medical University Vienna, Austria

Precise preoperative planning of approaches to intracranial lesions and correct intraoperative orientation during neurosurgical interventions rely on MR images in today's clinical practice. High-field strengths at 3T are currently used to display anatomy, function and metabolism with high-quality and high-resolution. Ultra high-field scanners at 7T may further improve the applicability of the MR image data for neurosurgery in future.

This lecture is based on the experience of the Department of Neurosurgery of the Vienna Medical University with high- and ultra high-field MR images and focuses on two examples:

1. Pituitary surgery: High-resolution display of the *anatomy* in perisellar compartments is crucial for the success of transsphenoidal endoscopic surgery of sellar lesions to evaluate possible invasion of the adenoma into cavernous sinus structures and to display important vascular and neural anatomy therein that has to be respected during surgery.
2. Glioma surgery: Due to their heterogenous nature, intratumoral areas of highest *metabolism* have to be selectively sampled for the correct histopathological diagnosis and the consecutive allocation to adjuvant treatments. Multivoxel MR spectroscopy (chemical shift imaging) has recently been successfully implemented for biopsy of such anaplastic foci. Due to the diffusely infiltrating nature of gliomas, neurosurgical resection of such tumors has to be limited in areas of important *function* to avoid permanent postoperative neurological deficits. Cortical functional areas and white-matter fibre tracts can be displayed intraoperatively from postprocessed MR data and aid the performing surgeon in judging the appropriate extent of tumor resection.

The concurrent display of multimodality MR image data of anatomy, metabolism and function by image fusion and/or segmentation and the possibility to display the images in multiplanar 2D mode or with 3D volume rendering further enhances the neurosurgeon's planning capabilities. The possibility to additionally navigate these image data greatly enhances orientation intraoperatively.

Evaluation of High-quality 3D Brain Surface Visualization for Brain Tumor Surgery

Aygül Mert, Georg Widhalm, Alex Micko, Gregor Kasprian, Daniela Prayer, Thomas Czech, Engelbert Knosp, Stefan Wolfsberger

Department of Neurosurgery, Medical University Vienna, Vienna, Austria

Objective: The aim of this study was to evaluate the advantages of high-quality three-dimensional (3D) brain surface visualization (BSV) over conventional two-dimensional (2D) magnetic resonance (MR) images for preoperative planning and intraoperative guidance.

Methods: 3D-BSV was performed in 60 cases (47 gliomas, 5 cavernomas, 5 meningiomas and 3 metastases). For brain surface reconstruction we used (1) T1-weighted MR images with and without contrast enhancement (CE) as anatomical surface information and (2) diffusion-weighted MR images as basis for brain volume extraction and segmentation. Postprocessing of MR images was performed on a PC-based workstation running the StealthViz® surgical planning software (Medtronic, CO, USA) which includes advanced segmentation and volume rendering modules. To assess the value of 3D-BSV for preoperative planning we created a multiple-choice-test for exact lesion localization and identification of gyral and sulcal anatomy. The test consisted of 20 cases and was conducted with 10 neurosurgical residents in different levels of training, once with standard 2D images in all 3 planes and then with 3D brain surface models. Median time for completion and success rate was calculated and compared between the 2D and 3D methods. The value of 3D-BSV for intraoperative orientation was determined, first, in the operating room by experienced neurosurgeons, who defined the relevance and accuracy of the 3D brain surface models

compared to the intraoperative image and second, by topographical correlation of particular anatomical structures such as superficial veins (≥ 1 mm in diameter) and gyri, which could be observed in the 3D brain models and the intraoperative images.

Results: The comparison between the 2D/3D multiple-choice-test showed a significantly higher success rate ($p=0.001$, X²) in the 3D test, while being significantly less time-consuming ($p<0.001$, X²). Intraoperatively, a significant correlation was found between the 3D images, superficial cerebral veins ($\geq 0,7$ mm in diameter) and gyral anatomy.

Conclusion: The 3D-BSV is a clinically reliable tool for preoperative planning, exact lesion localization and intraoperative guidance in brain tumor surgery especially for small subcortical lesions in eloquent areas. Therefore, it may be an excellent tool for training residents and young neurosurgeons.

Neuroimaging the Sequelae of Mild Traumatic Brain Injury

Andre Obenaus¹⁻⁴, Lei Huang², Stephen Ashwal³

Departments of Radiation Medicine¹, Biophysics and Bioengineering², Pediatrics³, Radiology⁴, Loma Linda University, Loma Linda, USA

Mild traumatic brain injury (mTBI) is an increasing medical concern for individuals engaged in active sports and military services. Recent guidelines for diagnosis of mTBI acutely include criteria that no observable changes within the brain be visible on standard neuroimaging (magnetic resonance imaging, MRI; computed tomography, CT). However, long-term neurological, neuropsychological testing supports the loss of brain function within mTBI patients. Neuroimaging, using emerging new approaches such as diffusion tensor imaging (DTI), suggest that there are significant changes within the white matter of the brain after mTBI. However, the underlying pathophysiology, particularly following repetitive mTBI is not well understood. Similarly effective therapeutics remain to be found for mTBI.

We developed a novel rodent model of mTBI to examine the spatial and temporal alterations within the brain using standard neuroimaging modality (T2-weighted) and newer approaches including susceptibility weighted imaging (SWI) for extravascular blood and DTI for white matter injury. Furthermore, we varied the interval between two episodes of repetitive mTBI events to examine if there was a period of vulnerability following initial mTBI. Finally, we assessed the ability of hyperbaric oxygen therapy (HBO) to ameliorate the pathophysiological sequelae of mTBI.

We found that a 3 day interval between repetitive mTBI worsened outcome measures (behaviour, lesion volume, extravascular bleeding). DTI revealed that a single mTBI induced axonal injury that was exacerbated by repeated mTBI. Tissue histopathology correlated with *in vivo* MRI findings in which repeated mTBI resulted in increased cortical tissue damage and astrogliosis. HBO pre-treatment (24 hrs prior to initial mTBI) or post-treatment (24 hrs post initial mTBI) improved neuroimaging outcomes following repetitive mTBI in contrast to those seen in tissues without HBO intervention. There were significant reductions in the lesion and hemorrhage volumes at 24 hrs post repetitive mTBI. The most dramatic neuroprotection by HBO was a 3-fold decrement in hemorrhage volumes back to Sham levels.

Collectively, our findings suggest that cumulative brain tissue damage occurs following repetitive mTBI including increased white matter vulnerability. Both prophylactic and therapeutic HBO provides a potential neuroprotective strategy that can be applied to individuals at high risk for repetitive mTBI. MRI is a sensitive neuroimaging biomarker for monitoring experimental and clinical treatment effects within the setting of repetitive mTBI.

Funding: This study was supported by funding from the Department of Defense (DCMRP #DR080470)

How about MRI in Space?

Krzysztof Turek

AGH University of Science and Technology
Faculty of Physics and Applied Computer Science, Department of Medical Physics and Biophysics
al. A. Mickiewicza 30, Kraków

The major aim of each MRI manufacturer is to produce the system generating the highest possible signal-to-noise and maximum spatial resolution within the shortest possible time. At the same time the size, weight and power consumption of the system are not of great importance. A concept of MRI on the International Space Station (ISS) supported by the Canadian Space Agency (1) requires a different approach due to weight, size and power consumption constraints associated with the system suitable for ISS. The shipment to the ISS cannot exceed 800 kg and its total dimensions must be less than 2014x1046x850 mm. Furthermore the power consumption must be low. Production of a system fulfilling these requirements is very challenging. The heaviest part of each MRI system is the magnet, which weight is in the range 4 tones, for 1.5 T superconducting magnet, and 17 tones for 0.35 T permanent magnet. The total weight of electronics is usually about 300 kg, 60% of which is the weight of gradient and RF amplifiers. With these figures in mind, it is hard to imagine, that the weight of a classical system could allow transportation of the MRI system to ISS. A solution seems to be a combination of two new technologies: (i) the lightweight Halbach magnet developed by AMAG – Dr Krzysztof Turek in Poland and (ii) the Transmit Array Spatial Encoding Radio Frequency (TRACE RF) developed by the National Research Council of Canada, Institute for Biodiagnostics (2,3). The first technology reduces drastically the weight of the magnet and the second one allows elimination of the heaviest and the most power consuming gradient coils and gradient amplifiers. Base on the theoretical calculations and preliminary tests it was found (4) that production of such a system is indeed possible. The results showed that a 0.15 T Halbach magnet system for the whole body MRI of the weight of only 700 kg and dimensions suitable for transportation to ISS could be constructed. The utilization of the gradient-free TRACE MRI (3) allows reduction of the total weight of the electronic components to below 100 kg. Thus the total weight of the entire whole body MRI system can be less than 800 kg.

The development of a system for MRI in the space would allow to explore the limits of MRI physics and technology. The space MRI system would be a powerful tool for astronaut's diseases diagnosis and treatment monitoring, as well as a registration of physiological changes due to zero gravity, such as bone losses. However what seems to be even more important is that the new technology could be utilized for developing light, portable and easy to use MRI systems for the use on Earth.

References

1. G. Sarty, University of Saskatchewan, private information.
2. S.B. King, et. al. Proc. ISMRM 2006, p.2628.
3. Sharp J.C., S.B. King, Magn Reson Med **63** (2010) 151-161.
4. Turek K. and Liszkowski P. Technical Report, AMAG-Dr Krzysztof, 2011.

Molecular Imaging: Nanobodies meet Nanoparticles

Abdelnasser Abulrob

National Research Council of Canada-Institute for Biological Sciences, Ottawa, Ontario, Canada

Molecular imaging is one of the most advanced platforms for biosensing that enables simultaneous determination of both anatomical localization and quantitative changes of target biomolecules or specific cells in a living organism. The development of techniques for the molecular imaging of tumours promises not only to distinguish cancerous from non-cancerous cells, but to provide information on molecular characteristics of malignant cells that can guide the selection of treatment protocols and provide means for monitoring their success.

The emergence of nanosynthesis technology provides new materials with distinct physical properties for a broad spectrum of imaging modalities. Some of these include

superparamagnetic particles for magnetic resonance imaging (MRI), and fluorescent quantum dots (QD) for optical imaging. However, all imaging modalities harbour intrinsic advantages and limitations. Therefore, nanoparticles with signal enhancement in dual or multiple imaging modalities are expected to become a significant trend in future biosensing technologies.

Our research focus is in 1) Synthesis of very high contrast sensing agents 2) The development of molecular targeting moieties that recognize disease-specific molecular markers/targets, 3) The development of biocompatible nanocarriers for in vivo targeting with remote sensing capabilities, and 4) The optimization of bioconjugation strategies and pre-clinical validation of these agents in animal models.

In my talk I will share with you our research in development of novel molecular imaging agents for detection of specific antigens in brain diseases and optimization of these agents in pre-clinical animal studies.

In Vivo Imaging of Integrin Over-expression in Rat Myocardial Infarction

L.Menichetti¹, C.Kusmic¹, D.Arosio², L.Manzoni², D.Panetta¹, M.Matteucci³, D.Petroni¹, C. Casagrande², P.A. Salvadori¹, A.L'Abbate³

¹CNR Institute of Clinical Physiology (Pisa), ² CNR Institute of Molecular Science and Technology (Milan), ³ Scuola Superiore Sant'Anna (Pisa)

Introduction: Angiogenesis plays a pivotal function in the repair process after an ischemic injury and has a relevant interest in cardiovascular research. Integrins are one of the major families of cell adhesion receptors mediating an array of cellular processes, including cell adhesion, migration, proliferation, differentiation, and survival. The specific $\alpha_v\beta_3$ integrin expressed by endothelial cells has been identified as a critical modulator of angiogenesis. In this study we used a specific library of cyclic RGD pentapeptide mimic based on azabicycloalkane amino acids that demonstrated high activity and selectivity for integrin $\alpha_v\beta_3$ in vitro. This library currently under development by our group, has been conjugated with ⁶⁸Ga-labelled NOTA derivative thereby enabling it for PET imaging. The goal of this study was to explore by microPET/CT the potential of this RGD scaffold in order to define the time course and the extent of integrin expression in a rat model of myocardial infarction.

Materials and Methods: 5 Rats underwent permanent ligation of the left anterior descending coronary artery and 3 were sham operated. All received intravenous administration of 75 MBq/kg of ⁶⁸Ga-NOTA-RGD at different times after the operation. Labelling was performed at room temperature with SPE purification; 98% radiochemical purity was checked by HPLC. Micro-PET images were acquired using the YAP-(S)PET scanner; micro-CT images were acquired with the Xalt-HR scanner, that is an engineered small animal CT scanner built in our laboratories. Coregistration between PET and CT images was performed by rigid geometric transformations. ROI for focal tracer uptake were defined on a mid-myocardial section in both ischemic and contro-lateral region of infarcted rats. The ROI definition was the same in sham-operated and infarcted animals. To correlate integrin expression with imaging signals we detected endothelial cells and integrin β_3 subunit by CD31 and CD61 immunohistochemical staining in the same hearts.

Results and Discussions: Focal ⁶⁸Ga-NOTA-RGD uptake was detected mainly in the basal portion of the left ventricle anterior wall. The best tradeoff between uptake ratio and image counting statistics was recorded at 90 minutes after injection: about twice the activity in the infarct area with respect to contra-lateral region was recorded. Optimal tracer uptake was found 3 weeks after the surgery. Preliminary data indicated an increased number of CD31 positive vessels, paralleled by a positive β_3 integrin staining especially at the border zone of the infarcted area. This study demonstrated the feasibility of ⁶⁸Ga-NOTA RGD radioligand in investigating the myocardial integrin expression by PET / CT approach in a small animal infarct model. PET imaging of the new ⁶⁸Ga-NOTA-RGD could be then investigated as a promising tool for non-invasive monitoring of therapeutical intervention aimed at stimulating angiogenesis in ischemic heart disease.

Bioimaging Modalities in Discovery and Validation of Biomarkers for Brain Diseases

Danica Stanimirovic

Institute for Biological Sciences, National Research Council of Canada

The brain is a highly complex organ, both anatomically and physiologically; modern advances in brain imaging – from nanoscale molecular imaging of cells to functional MRI imaging in patients – offer the opportunity to elucidate the integrated molecular and functional complexity of the brain. Imaging technologies are important in aiding the fundamental understanding of the brain and neurovascular function and are among key enablers of discovery translation into commercial and clinical applications. Imaging techniques are now capable not only of visualizing chemically diverse biologically active species compartmentalized in discrete regions of the brain, but also of measuring the dynamics of their appearance and activity.

This lecture will review a spectrum of bioimaging modalities used for discovery and validation of biomarkers in brain diseases, ranging from imaging mass spectrometry to *in vivo* molecular imaging. Specifically, the lecture will focus on molecular imaging of cerebrovascular biomarkers. Brain vasculature is affected by and functionally implicated in a majority of brain diseases including among others stroke, Alzheimer's disease, multiple sclerosis and brain tumors. Changes in molecular 'make-up' (or functional properties) of brain vasculature are often early 'signs' of the brain disease that could be exploited as molecular imaging targets. A paradigm and examples of cerebrovascular biomarker discovery and validation which links genomics and proteomics discovery workflows with the development of single-domain antibody-based molecular imaging agents and their evaluation by non-invasive imaging *in vivo* will be presented. Validated cerebrovascular biomarkers could become surrogates for patient stratification and efficacy monitoring, reducing the length and cost of clinical trials.

Molecular MRI: a New Modality on its way into Clinical Routine

Jens-Christoph Georgi

Siemens Healthcare, Erlangen, Germany

Based on years of preliminary work with four PET head inserts, the so called BrainPETs, for the 3 Tesla MR system MAGNETOM Trio, with Biograph mMR™ Siemens now introduces the first system worldwide to combine the advantages of MRI with the strengths of PET.

Compared to a PET-CT system, the PET detector ring, which is exactly at the level of the magnet isocenter, had to be adapted so that its operation would not be disturbed by the strong constant magnetic field (3T) or the gradient fields of the MR scanner and that it would not interfere itself with these fields. A critical component typically used in PET-CT systems, the photomultiplier tube (PMT), is severely disturbed by the constant magnetic field of the MR scanner. Drawing on experiences made with the BrainPET prototype, this problem was solved by replacing the PMT with avalanche photodiodes (APD). Their advantage is that they are not only insensitive to the magnetic fields, but also considerably smaller than the PMT. Thus, it was possible to implement a magnet bore of 60 cm after integrating the PET detector ring into an MR scanner.

The PET detector also sets entirely new standards by its size in the axial (z) direction: with a FoV of 258 mm, it is the longest industrially manufactured PET detector. This offers a dual advantage: due to the large coverage, fewer bed positions need to be acquired in multi-bed exams. In addition, the large solid angle covered allows for a very high volume sensitivity (13.2 cps/kBq) which translates directly into low-noise images.

On the MR side, too, the system is a state-of-the-art 3T system with the same gradient specification as all the other Siemens 3T MR scanners (45 mT/m, 200 T/m/s). Together with the mMR local coils especially optimized for simultaneous MR and PET imaging, it is possible to perform not only the standard imaging sequences, but also all the advanced functional MR sequences to be combined with PET imaging: BOLD, diffusion-weighted MRI, MR spectroscopy, DTI and fiber tracking - all this across the whole body and, due to the Tim (Total Imaging Matrix) coil technology, without changing coils or repositioning the patient.

Based on experiences gained with the BrainPET scanners, it was also possible to solve the problem of photon attenuation and scatter in PET imaging. An automatic attenuation and scatter correction for PET images based on special MR sequences that are acquired simultaneously with the PET data is performed.

In addition to its low space requirement, an integrated system also offers considerable advantages in clinical operation. Acquiring a single exam with an integrated system, controlled by one technologist via one control unit, dispenses with the necessity of coordinating two examination dates for two systems in different departments also leading to faster examination results for patients.

Simultaneous MR and PET imaging opens up entirely new possibilities with regard to image quality and thus diagnosis: precise spatial and temporal registration of anatomical, functional and metabolic image data, simultaneous acquisition of PET and MR data for attenuation correction, or MR imaging for motion correction in the PET data.

What Contributions can MRI make for Non-invasive Cell Tracking?

Uwe Himmelreich

Biomedical NMR Unit/ MoSAIC, Katholieke Universiteit Leuven, Belgium
(uwe.himmelreich@med.kuleuven.be)

MRI is one of the most powerful tools for high-resolution, non-invasive imaging. Apart from monitoring anatomical and functional changes, the location and migration of cells can be followed by MRI. Current limitations of cell imaging by using MRI include unspecific contrast for iron oxide labeled cells, lack of information on the functional status of the cells and cell viability. Such shortcomings are traditionally overcome by combining MRI with other imaging modalities like bioluminescence imaging or positron emission tomography. Recent developments have shown that using responsive MR contrast agents or non ^1H based MRI/ contrast agents also provide functional information and improve specificity, respectively.

Our work focuses on the optimization of cell labeling strategies for robust, sensitive and potentially quantitative visualization of stem and progenitor cells in therapy models *in vivo* to assess cell behavior after engraftment. The sensitivity, stability, toxicity and adverse effects on the cell biology by the labeling procedure were studied for iron oxide based particles. The potential of Gd-chelates and ^{19}F labeled compounds for cell labeling has been assessed *in vitro* and *in vivo*.

Although, the actual labeling procedure can be straight forward, there are several issues that require careful consideration for (stem) cell labeling and their *in vivo* applications. Among these issues are:

- (1) Generation of highly sensitive contrast for the visualization of small cell numbers
- (2) (Semi)quantification of cell numbers *in vitro* and *in vivo*
- (3) Generation of unambiguous contrast that distinguishes cells from other sources of hypo- or hyperintensity in MR images
- (4) Stable binding/ uptake to avoid leakage or transfer of contrast to other cells
- (5) Prevention of toxicity or alterations of cellular processes by the contrast agent
- (6) Minimal influence on the physiological behavior of the cells in the host
- (7) Generation of contrast even after continued cell proliferation

Apart from commercially available agents, we have tested in-house produced magnetoliposomes (functionalized and non-functionalized); Gd-chelates responsive to enzyme expression as well as ^{19}F -labeled agents that target specific cell types (for example GLUT-2 expressing cells like hepatocytes or beta-cells).

Literature: [1] Soenen SJ et al. (2011) WIREs Nanomed Nanotech 3: 197-211. [2] Soenen SJ et al. (2011) Biomaterials 32: 1748-1758, [3] Soenen SJ et al. (2010) Small 6: 2136-2145, [4] Himmelreich U & Dresselaers T (2009) Methods 48: 112-124.

Adipose Tissue is a Potential Source of Multipotent Stem Cells for Treatment of Heart Failure

Ganghong Tian

Institute for Biodiagnostics, National Research Council Canada, Winnipeg, Manitoba, Canada

Heart failure is the leading cause of death worldwide. Unfortunately, current therapies are unable to stop the pathological cascade of heart failure. Recent studies have shown that stem cells may be an effective therapeutic strategy for curing of the devastating disease. However, ideal cell types for treatment of heart failure and other degenerative diseases have not been defined.

Adipose tissue contains a type of adult stem cells, named "adipose-derived stem cells (ASCs). In our preclinical studies, we have found that ASC can differentiate into several cell lineages and express various growth factors that are essential for tissue regeneration. The results indicate that ASC has a great potential for use in clinic for treatment of heart failure and other degenerative disease. In my presentation, I will summarize our preclinical work on characterization and evaluation of ASC, particularly on their ability in repairing injured heart muscle.

In addition, effective cell therapy requires more than injection of right type of cells. Its outcome profoundly depends on whether stem cells are viable and functional after transplantation. Reliable monitoring of implanted stem cells *in vivo* is very important to understand the mechanisms of cell therapy and to maximize its therapeutic benefits. Magnetic resonance imaging offers a great spatial resolution while positron emission tomography (PET) offers a great sensitivity, allowing detection of chemicals in a picomolar level. Dual-modal probes that be visualized by MRI and PET would therefore have a wide research and clinical application in stem cell therapy, cardiology, oncology, and neurology. In my presentation I will briefly talk about our studies on monitoring of stem cells using both PET and MRI. I will also mention our work on development of dual-imaging nanoparticles for tracking stem cells.

Intermolecular Effects in ^3He and ^{129}Xe NMR Spectra

Karol Jackowski¹, Michał Jaszuński², Bohdan Kamiński², Marcin Wilczek¹

¹Laboratory of NMR Spectroscopy, Faculty of Chemistry, University of Warsaw, Pasteura 1, 02-093 Warszawa, Poland

²Institute of Organic Chemistry, Polish Academy of Sciences, Kasprzaka 44, 01-224 Warszawa, Poland

Helium-3 and xenon-129 are well-known in the field of nuclear magnetic resonance (NMR) spectroscopy. They are both noble gases with spin $\frac{1}{2}$ and therefore can be applied to the wide range of research work. In particular optical pumping methods can increase the nuclear spin polarization of ^3He or ^{129}Xe by several orders of magnitude, thereby enhancing their NMR signals what is especially important for magnetic resonance imaging (MRI) experiments. However the physical and chemical properties of helium and xenon are significantly different. Xenon is already frozen at liquid-nitrogen temperatures, its liquid phase may be obtained at moderate pressure (e.g. 10 bar) via condensation at 200 K. Helium-3 can be liquefied at about 4.2 K at 1 bar. Moreover helium has a self-diffusion constant roughly 30 times that of xenon. As seen helium-3 is available for NMR investigations mostly in the gas phase while xenon can be also used as the excellent liquid solvent, its supercritical phase can be attained under relatively mild conditions. Xenon has also its own chemistry and forms inclusion complexes with various organic molecules like α -cyclodextrin. It is consequently understood that xenon has also anesthetic properties. Since helium-3 is chemically and physiologically inert, it is successfully used in MRI to study the pneumatics of lungs. There is only one problem, helium-3 is terribly expensive (3500 EUR per one liter), its supplies are limited and

at present it is rather difficult to get it at any cost. We should ask if it is possible to use xenon-129 as the alternative molecular probe in MRI studies.

In our laboratory we apply gas-phase ^3He NMR experiments for the direct measurement of shielding constants of other magnetic nuclei [1-3]. The procedure is as follows: NMR resonance frequencies are observed as the function of density and the results of measurements are extrapolated to the zero-density point. As the density dependence is linear the extrapolation gives us exact information on NMR parameters (frequencies or shielding constants) free from intermolecular interactions and the slope of this function allow the measurements of intermolecular effects in the gas phase. This way we can quantitatively compare the intermolecular effects directly observed for ^3He and ^{129}Xe atoms and also for many other different molecules when helium and xenon are used as the gaseous solvents. In every case we could find large difference in the intermolecular effects observed for shielding of ^3He and ^{129}Xe nuclei. Similar results were obtained when helium and xenon were used as the gaseous solvents and shielding of other molecules was monitored. Xenon generally produces distinct intermolecular effects, sometimes larger than observed for molecules. It proves that large xenon atoms can not substitute helium when the inert molecular probe is needed for MRI.

[1] Jackowski K., Jaszuński M., Wilczek M., J. Phys. Chem. A, **114**, 2471-2475 (2010).

[2] Jackowski K., Jaszuński M., Kamieński B., Wilczek M., J. Magn. Reson., **193**, 147-149 (2008).

[3] Jackowski K., Jaszuński M., Concepts Magn. Reson. A, **30A**, 246-260 (2007).

Beyond Boltzmann: Hyperpolarized Color MRI

Jan-Bernd Hövener

University Medical Center Freiburg, Department of Radiology, Medical Physics

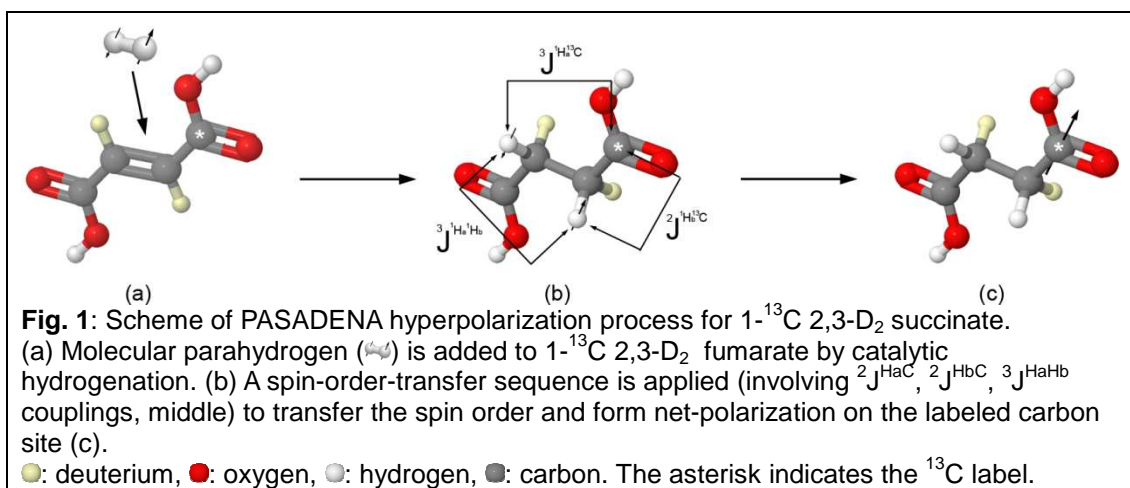
Magnetic Resonance (MR) has proven extremely powerful in various scientific braches including physics, chemistry and biology. Despite its success, however, much of its potential for medical application is yet unused. This is attributed to the inherently low sensitivity: only a miniscule fraction called polarization $P_{therm} \approx 10^{-6}$ of all nuclei contributes to the actual MR signal under *in-vivo* conditions (i.e. $T = 310\text{ K}$, $B \approx 3\text{ T}$).

Promising applications cannot be realized lacking sufficient signal. These include the real-time detection of metabolic changes of small samples like cells, for example to monitor treatment response.

Notable efforts are undertaken to increase the MR-signal, e.g. stronger B_0 , super-conducting coils or parallel imaging. However, most methods are limited to an enhancement of about one order of magnitude.

Hyperpolarization methods circumvent the thermal distribution altogether. Various "tricks" are used to achieve polarization of the order of unity, - an increase in nuclear alignment and MR signal of about five orders of magnitude without a background signal. The generation of ^{13}C -hyperpolarized molecules in solution and its application to biomedical MR has gained much interest recently.

Here, we present our approach to the hyperpolarization of ^{13}C biomolecules using parahydrogen, aiming at new hitherto inaccessible diagnostic parameters. We report our experiences in setting up a parahydrogen hyperpolarization lab (Fig. 1), hoping this will be helpful for other groups considering to enter this field of research.



Methods of Hyperpolarization

Paweł Grieb

Department of Experimental Pharmacology, Mossakowski Medical Research Centre, Polish Academy of Sciences, Warsaw, Poland

NMR signal intensity is proportional to the nuclear spin polarization, which at thermal equilibrium and external magnetic field B_0 of a few Tesla reaches few ppm only. MR techniques based on equilibrium polarization are therefore limited by low signal/noise ratio and low sensitivity. In the *in vivo* studies high quality ¹H MR images can be recorded because the signal comes from ortho-hydrogen nuclei concentration of which is ca. 80 mol/L. However, even in most advanced *in vivo* ¹H MR spectroscopy experiments, signals from a limited number of substances (metabolites) attaining concentrations of 0.1-10 mmol/L can only be recorded. Moreover, while in principle imaging and spectroscopy of heteronuclei (eg. ¹¹C, ¹⁵N) could be used, their low natural abundance and low gyromagnetic ratio make such approaches impractical.

Equilibrium polarization can be enhanced by increasing the applied external magnetic field B_0 and by decreasing temperature, but for *in vivo* applications the former is prohibitively expensive and the later not feasible. An alternative approach is to create a nonequilibrium prior to MRI/MRS investigation. Four methods have been described allowing to attain sample hyperpolarization: (i) the “brute force” approach in which sample is maintained (in the presence of a removable “relaxation switch”) at ultra-low temperature and very high B_0 for a time sufficient to become hyperpolarized; (ii) the “optical pumping” (applicable only to ³He and ¹²⁹Xe) in which electrons of an alkali metal (Rb) or a metastable ³He vapor are polarized by laser light and their polarization is transferred to the atoms of noble gas; (iii) the “parahydrogen induced polarization” (PHIP, also named PASADENA) in which H₂ is enriched in the para form at low temperature in the presence of a suitable catalyst and non-equilibrium population of p-hydrogen molecules is chemically reacted with substrates having C=C bonds to yield molecules with strongly enhanced absorption/emission NMR signals; (iv) the “dynamic nuclear polarization” (DNP) in which sample doped with a stable free radical (eg. tempol or trityl) is dissolved in a glass-forming solvent, placed in the steady magnetic field, frozen to 1°K and irradiated by appropriate radiofrequency, resulting in polarization of electrons and its subsequent transfer to nuclei in sample; sample is then dissolved and transferred into NMR spectrometer or injected into organism. These methods have potential to amplify MR signals arising from sample constituents 20,000-100,000 fold, although hyperpolarized state is transient and (in most cases) quickly decays due to relaxation.

Hyperpolarization allows for a number of previously unforeseen applications of MR which may soon find way into clinical routine. Inhaled hyperpolarized noble gases can be used to image both airspace anatomy and apparent diffusion coefficient in lungs, allowing early and accurate diagnosis of chronic pulmonary obstructive disease. In animal experiment inhalation of hyperpolarized ³He has recently been shown to accurately detect lung cancer micrometastases through imaging superparamagnetic iron oxide nanoparticles (SPION)

functionalized with cancer-binding ligands and given intravenously. Spectroscopic imaging following intraarterial injections of ^{13}C -containing metabolites (such as pyruvate and malate) hyperpolarized by DNP allows detection and quantitation of cellular damage in post-ischemic brain or heart, as well as very early assessment of tumor response to chemotherapy. In the future hyperpolarization of metal ions (eg. ^6Li , ^{89}Y) which may be chelated, or ^{29}Si in silica nanoparticles which exhibit multi-hour spin relaxation times, may open further perspectives for convenient MR imaging of various molecular targets of clinical importance.

MEOP Polarisation of ^3He for Clinical Lungs Imaging

Tadeusz Pałasz

Institute of Physics, Jagellonian University

The hyperpolarized ^3He gas can be used as an inhaled contrast agent in Magnetic Resonance Imaging of human lungs. One of the methods to obtain high magnetic polarization of ^3He gas is Metastability Exchange Optical Pumping (MEOP), which is usually performed at low pressure (~ mbar) and at low magnetic field (~ mT). MEOP method can be also performed at higher gas pressure and at high magnetic field. The prototype of the first high field in-situ polariser, working inside a commercial 1.5 T scanner and images of human lungs filled with ^3He polarised using this method will be presented.

Clinically Accurate Cancer Diagnosis by MR Spectroscopy

Ian C.P. Smith[†], Ray L. Somorjai[†], Tedros Bezabeh[†], Omkar B. Ijare[†], Carolyn E. Mountford*

[†]Institute for Biodiagnostics, National Research Council, Winnipeg, Canada

*Department of Radiology, Harvard University, Boston, USA

Cancer diagnosis is traditionally done by anatomical and pathological methods. However, both those characteristics are determined by the underlying cellular activity. Therefore, direct, minimally invasive estimates of cellular metabolites should yield a positive diagnosis in the earliest stages of the cancer evolution. This process is what we call cancer metabolomics, the signature of the genetic alteration, which we do by ^1H NMR spectroscopy.

A first example is the biliary tree – liver, gall bladder, pancreas. The simplest method to measure metabolites is high resolution NMR of solutions of bile. These yield a large number of resonances, which can potentially separate patients with primary sclerosing cholangitis with or without cancer of the bile duct or liver. With cancer, the usual treatment by liver transplant is futile. To determine the most discriminating features of the spectra, and to provide robust diagnostics, we have developed a Statistical Classification Strategy (SCS).¹ In most cases, it yields accuracies of 90-100%, and is robust to all incoming samples.²

Bile is normally obtained by endoscopy – a probe traverses the digestive tract and enters the bile duct - a relatively invasive procedure. Our success with isolated bile led us to perfect a technique to obtain NMR spectra of bile *in vivo*, by focusing on the bile in the gall bladder in a hospital type MRI instrument. We are now obtaining high quality spectra at 125 MHz (3 Tesla) and undertaking a clinical study in order to develop a robust, non-invasive, clinical technique.

A second example is a means to determine if a breast tumour has spread to the rest of the body. This we do by obtaining the ^1H MR spectrum of a fine needle biopsy taken from the primary tumour. By means of our SCS we can easily classify these with accuracy of nearly 100% as either cancer or benign.³ Taking only the samples classified as cancer, we can separate them into two classes, contained or released to the body (metastasized), with an accuracy also of 100%. Knowing that the tumour is contained relieves the patient from the trauma and inconvenience of having the lymph nodes under the arm removed for analysis and from possible swelling for the rest of her life, and gives a more accurate measure of whether the tumour actually has spread. Similar results have been obtained with colon cancer.⁴

Our success in these examples depends strongly upon the elegant SCS developed by Ray Somorjai. Details of the method will be presented in his talk.

¹ ICP Smith and RL Somorjai, *Biophys. Rev.* **3**, 47-52 (2011)

² N Albiin et al, *Acta Radiol* **49**, 855-862 (2008)

³ CE Mountford et al, *Brit. J. Surgery* **88**, 1234-1240 (2001)

⁴ T Bezabeh et al., *NMR Biomed* **22**, 593-600 (2009)

Classification-based Accurate and Robust Diagnoses of Complex: An Essential Step Towards Clinical Use

Ray Somorjai, Ian C.P. Smith

Institute for Biodiagnostics, National Research Council, Winnipeg, Canada

The ultimate goal of developing classifiers for biomedical data, obtained by non-invasive methods, such as NMR spectroscopy, is to transfer the instrument/classifier methodology to the clinic. The bottleneck is the lack of robust, reliable classifiers, i.e., classifiers that can diagnose spectra obtained from patients with unknown pathology with high class assignment confidence. The major obstacles are the twin curses of **high dimensionality** (too many dimensions (data points, features), $O(1,000) - O(10,000)$) and **dataset sparsity** (not enough samples, $O(10) - O(100)$).

We shall first sketch earlier spectroscopic approaches (based on “visual inspection”, or using conventional classifiers, such as Partial Least Squares), and compare them with classifiers created via our 5-stage **Statistical Classification Strategy** (SCS). The SCS was inspired and developed by recognizing that there is no single, best classifier methodology, i.e., classifier development must be data-driven.

The five stages of the SCS comprise visualization, preprocessing, feature selection/generation, classifier development and classifier aggregation. We shall focus on visualization and feature generation, and outline how their improvement helps creating powerful, yet conceptually transparent classifiers.

Visualization may be achieved by projection/mapping from the originally high-dimensional feature space down to two or three dimensions. The method we have developed we call **Class Proximity Projection, CPP**. For each sample of the dataset it produces two distance-dependent coordinates. Their characteristics are controlled by a pre-selected **class proximity measure π** (e.g., the class centroids) and a **dissimilarity/distance measure Δ** (e.g., Euclidean). Various combinations of the π/Δ pair impart great flexibility to classifier generation via the CPP, with readily visualizable outcome. As a bonus, preprocessing is much simpler (e.g., binning adjacent spectral points is frequently sufficient). Furthermore, aggregation of radically different classifiers becomes easy.

We demonstrate CPP's use on ¹H MR spectra, obtained for colon, bile, and breast cancer. For all datasets we achieved well-balanced, high (90-100%) sensitivities and specificities.

We thank Drs. T. Bezabeh and O.B. Ijare for producing the ¹H MR spectra for the bile and colon cancer data, Dr. C.E. Mountford and her team for the breast cancer spectra and Mr. B. Dolenko and Dr. A. Nikulin for realizing the algorithms necessary for creating the (still evolving) CPP software.

References:

Somorjai, R.L., Dolenko, B., Nikulin, A., Roberson, W., Thiessen, N., **Class proximity measures – Dissimilarity-based classification and display of high-dimensional data.** *J Biomedical Informatics* (2011) in press; doi:10.1016/j.jbi.2011.04.004.

Somorjai, R.L., Alexander, M., Baumgartner, R., Booth, S. *et al.*, **A Data-Driven, Flexible Machine Learning Strategy for the Classification of Biomedical Data.** Chapter 5 in: *Artificial Intelligence Methods and Tools for Systems Biology* (Dubitzky W and Azuaje F,

(eds.)), Computational Biology Series, Vol. 5 Springer pp. 67-85 (2004).

Somorjai, R.L., Dolenko, B., Mandelzweig, M., **Direct Classification of High-Dimensional Data in Low-Dimensional Projected Feature Spaces Comparison of Several Classification Methodologies.** *J Biomedical Informatics*, 40, 131-138 (2007).

Inflammation and Disease: Opportunities for Imaging

Daniel A. Muruve

Department of Medicine, Immunology Research Group, Institute of Infection, Immunity and Inflammation, University of Calgary, Calgary, AB, Canada

Inflammation accompanies most acute and chronic diseases. Inflammation can be induced by a wide range of microbial and non-microbial stimuli that contributes to disease pathogenesis and patient morbidity and mortality. Therefore, inflammation is a very attractive and significant target for therapeutic and diagnostic intervention in humans. Over the past decade, the innate immune system has been recognized to play a larger role in the pathogenesis of inflammation and immune responses associated with disease. As an example, the Nod-like receptors or nucleotide binding domain leucine rich repeat containing (NLR) family of genes play an important role in the development of innate immune responses and are associated with numerous pro-inflammatory human diseases. These conditions involve many organ systems and include arthritis, neurodegenerative disorders, metabolic disorders (obesity and diabetes), cardiovascular disease (atherosclerosis, myocardial infarction), inflammatory bowel disease, acute and chronic kidney disease and hypersensitivity dermatitis. A brief overview of the pathogenesis of the innate immune system in inflammation and disease will be provided. Cellular and molecular markers of innate immune activation that might be amenable to diagnostic imaging techniques will be discussed in addition to some of the animal models that are available for pre-clinical proof-of-principle studies.

Study of the evolution of HPMC Based Matrix Systems During Hydration using 1H MRI

Piotr Kulinowski¹, Przemysław Dorożyński², Anna Młynarczyk¹, Krzysztof Jasiński¹, Bogusław Tomanek^{1,3}, Władysław P. Węglarz¹

¹Department of Magnetic Resonance Imaging, Institute of Nuclear Physics PAN, Krakow, Poland,

²Department of Pharmaceutical Technology and Biopharmaceutics, Jagiellonian University, Krakow, Poland,

³Institute for Biodiagnostics, National Research Council of Canada, Winnipeg, Manitoba, Canada

Hydroxypropymethyl cellulose (HPMC) belongs to best recognized excipients applied for preparation of controlled release polymeric matrix systems. Wide range of types of the polymer and repeatability of samples, make HPMC the polymer of choice for formulation of controlled release systems.

Structure and evolution of the polymeric matrix loaded with drug can supply additional data for further, comprehensive analysis of the system behavior. MRI can be performed in the flow-through cell according to Pharmacopoeial USP4 standard assuring sink condition [2]. The structure can be assessed during drug dissolution test in USP4 apparatus from T1/T2 weighted magnitude images. As an example, commercial quetiapine fumarate matrix tablets were studied. Histogram based image segmentation was performed according to triple-modal image intensity distribution [1]. The regions were assigned as a dry glassy core region, interface layer and gel layer.

The most interesting, rarely identified and discussed, region is interface layer [1,3]. To better characterize its structure during hydration, MRI microscopy (T2 and T1 relaxometry) was performed with spatial resolution of 59 μm. L-dopa and ketoprofen were used as model drugs of different solubility. Solubility difference between drugs was chosen to be in order of magnitude. Differences in structure and its evolution between the HPMC matrices loaded with L-dopa and ketoprofen were shown. In consequence, five different regions (i.e. dry glassy, hydrated solid like region, two interface layers and gel layer) were identified vs. two or three as obtained in previous studies [1,3,4,5].

The work was supported by the Polish Ministry of Science and Higher Education grant N N518 407438.

References:

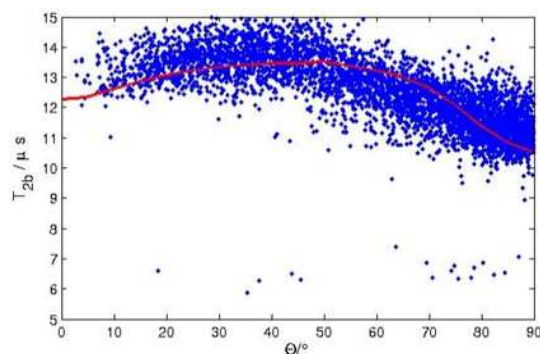
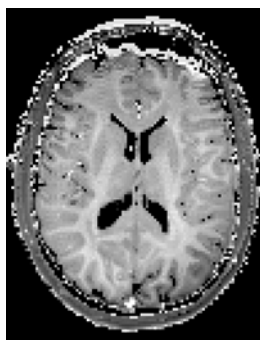
- [1] Kulinowski P, Dorożyński P, Młynarczyk A, Węglarz WP. *Pharm. Res.* 2011;28(5):1065-73.
- [2] Nott K. *Magnetic resonance imaging of tablet dissolution. Eur J Pharm Biopharm.* 2010;74:78–83.
- [3] Kojima M, Ando S, Kataoka K, Hirota T, Aoyagi K, Nakagami H. *Chem Pharm Bull.* 1998;46:324–328.
- [4] Tajarobi F, Abrahamsén-Alami S, Carlsson AS, Larsson A. *Eur. J. Pharm. Sci.* 2009;37: 89-97
- [5] Kowalczyk J, Tritt-Goc J, Piślewski N. *Solid State Solid State Nucl. Magn. Reson.* 2004; 25: 35–41

Orientation Dependence in Magnetization-transfer Imaging of Human White Matter

Harald E. Möller, André Pampel, Dirk K. Müller

Max Planck Institute for Human Cognitive and Brain Sciences, Leipzig, Germany

The proton signals from macromolecules and membranes are not directly visible to clinical magnetic resonance imaging (MRI) because their associated transverse relaxation times are on the order of 10 μ s. However, information can be obtained indirectly from magnetization-transfer (MT) experiments using off-resonance saturation of the broad macromolecular resonance line (semi-solid pool 'b') and observation of the effect on the free water (liquid pool 'a') [1]. Recently, we observed an orientation dependence of MT parameters in human white matter [2]. In particular, the transverse relaxation time of the semi-solid pool, T_{2b} , revealed noticeable structural contrast correlating with the orientation of major fiber bundles (Fig. 1). This dependence is even more evident in a voxel-by-voxel plot as a function of orientation. In general, orientational anisotropy of relaxation times or diffusion coefficients in biological tissues is well established revealing interesting aspects of tissue microstructure [3]. However, previous analysis had suggested that it is unlikely to observe MT anisotropy. This discrepancy can be resolved using a refined lineshape function to model the semi-solid pool 'b'. In quantitative analysis of MT data from brain tissue, a super-Lorentzian lineshape is commonly used [4]. It is expected to arise from dipolar interactions in partially ordered materials, in particular lipid bilayers [5] and results form a superposition of Gaussian lines. The Gaussian linewidths are scaled by a factor depending on the angle between the bilayer normal and the external magnetic field, \mathbf{B}_0 . This model inherently assumes an isotropic distribution of orientations. However, this condition is not fulfilled in large white-matter fiber bundles, where lipid bilayers are wrapped around the axons. We derived a novel lineshape describing a system of bilayers wrapped around axons oriented at an angle θ with respect to \mathbf{B}_0 . It resembles features of a super-Lorentzian shape if θ exceeds 35°, whereas it becomes Gaussian-like below this threshold. Instead of an unlikely perfect alignment of all fibers, a Gaussian distribution (standard deviation 20°) of orientations within a voxel was assumed. Despite some subtle deviation at large θ , a striking consistency between model and experimental data is achieved.



References

- [1] S.D. Wolff, R.S. Balaban. Magn. Reson. Med. 1989; 10: 135-144.
- [2] D.K. Müller, A. Pampel, H.E. Möller. Proc. ISMRM 2010; 18: 2996.
- [3] R.M. Henkelman, G.J. Stanisz, J.K. Kim, M.J. Bronskill. Magn. Reson. Med. 1994; 32: 592-601.
- [4] C. Morrison, R.M. Henkelman. Magn. Reson. Med. 1995; 33: 475-482.
- [5] H. Wennerström. Chem. Phys. Lett. 1973; 18: 41-44.

Image-guided Robotics in Neurosurgery

Garnette Sutherland

Diffusion MR Techniques in Tissue Microstructure Investigation

Mihaela Onu

University of Medicine and Pharmacy, Bucharest, Romania
 Clinical Hospital „Prof. Dr. Th. Burghele”, Bucharest, Romania

Diffusion magnetic resonance imaging and tractography are non-invasive tools to obtain information on the neural architecture, in vivo, of the human brain white matter (WM). These techniques are not only used to study brain macrostructure and pathophysiology but they can also characterize tissue microstructure.

Diffusion tensor imaging (DTI), which is the most popular tractography technique, allows reconstruction of neuronal fibers. However, DTI suffers from inherent artifacts and limitations. The main drawback is the inability of the model to cope with non-Gaussian diffusion.

Several models have been developed to overcome this limitation. The characteristics of these proposed models (Diffusion Kurtosis Imaging (DKI), Diffusion Spectrum Imaging (DSI), CHARMED) will be briefly reviewed in the presentation. It is possible to obtain more information on tissue microstructure from diffusion signal measurement, if non-Gaussian diffusion is assumed. Diffusion Kurtosis Imaging is able to offer images of the two WM compartments, the intraaxonal space (IAS) and extra-axonal space (EAS). CHARMED and its variant, AxCaliber offer a non-destructive, high accuracy quantification of axonal architecture in terms of mean axon diameter. Correlation between histologic and experimental mean axon diameter using AxCaliber model will be mentioned in the presentation.

In DTI technique, the reduction of anatomical information to a tensor and then to a scalar value (FA, MD, individual diffusivities) implies that when changes or differences are found in one of the scalar metrics, it is often difficult to draw any conclusions about the exact cause at the cellular level. In spite of numerous studies using DTI and histology observation, it has not been elucidated what mechanisms are underlying, for example, the changes in radial diffusivity, in neural studies: the breakdown of the axolemma or a change in its permeability, loss of neurofilaments and microtubules, axonal swelling or an increase in the extracellular space. However, when used in conjunction with other techniques such as Magnetization Transfer (MT), DTI can offer valuable information on cellular level like quantifying the myelin water content.

Despite its simplicity, the single tensor model (DTI), remains the most popular model adopted in clinical research where healthy and patient groups are compared.

UHF Imaging Update

Franz Schmitt

Siemens Healthcare, Erlangen, Germany

The intrinsic improvements in signal to noise ratio, spectral dispersion and susceptibility contrast with increasing static magnetic field strength, B_0 , has spurred the development of MR

technology from its very first application to clinical imaging of today. With maturing magnet, RF and gradient technology, the clinical community has seen the static magnetic field of clinical systems increase from 0.2T to 1.5T to 3.0T. Today, the "Ultra High Field" label for human MR research describes initial experiences with 7T, 8T and 9.4T systems.

At the time being there are 37/33 UHF/7T systems installed and further 19/15 UHF/7T system projects in work. The demand for UHF is increasing over the last years with more than 5 projects per year. While currently primarily research instruments, this technology is bound to cross the boundary into the clinical diagnostic arena as key technical issues are solved and the methodology proves itself for addressing clinical issues.

In this talk, we discuss the particular advantages and disadvantages of ultra-high field systems for clinical imaging as well as some of the immediate technological challenges which must be solved to derive the full benefit of the extraordinary sensitivity of these systems which has been glimpsed from their research use.

MRI RF Coil Design for better SNR, Speed and Excitation

Scott King

Institute for Biodiagnostics, National Research Council,, Winnipeg, Canada

Introduction

Receive Array Coils:

The number of receive channels on standard clinical MRI systems is between 8 and 32, but now reaching as high as 128, allowing the possibility for highly accelerated parallel MRI and increased SNR. To maximize MRI speed and SNR and spatial resolution, phased array optimization is needed, through both simulation and experimentally. To lessen the demands for data handling and processing, data compression methods [1-4] can be explored in hardware, such as eigenmode data compression, capable of N/2 compression maintaining 100% SNR.

Transmit RF Coils:

Due to RF wave behavior and sample interaction at high B₀ fields, B₁⁺ shimming aiming at uniform excitation is important for improved SNR and image uniformity, while avoiding complicated 2D spatially selective RF methods. Most methods have focused on optimizing the current distribution in a typical birdcage structure, but this alone is not sufficient as variation in the current distribution along the z-axis is required [5]. Improved B₁ homogeneity can be achieved by varying the phase of the B₁ field in the z-direction using a spiral birdcage design [6]. Such "phase gradient" RF coils are also required for a new RF-only MRI method [7] that benefits from a uniform B₁⁺-magnitude distribution. Another alternative is to use a multi-transmit array, which can allow B₁⁺ shimming adjustable to the individual subject, and further allow acceleration (shorter pulses) for complicated 2D or 3D RF pulse excitations (Tx-SENSE).

Synopsis

Software and hardware methods used in Rx and Tx RF coil optimization will be discussed, along with results of array optimizations, improved homogeneity RF coil designs, and Tx-SENSE results on a 3T Tx-array system.

References

- [1] King SB, et. al. Concepts Magn Reson Part B (Magn Reson Eng) 2006; 29B(1): 42-49.
- [2] King SB, et. al, Magn. Reson. Med. 63:1346–1356 (2010).
- [3] Alagappan V, et.al.. Magn Reson Med 2007; 57:1148–1158.
- [4] Buehrer M, et.al.. Magn Reson Med 2007; 57:1131–1139.
- [5] King et al, ISMRM 2009 p.390.
- [6] Alsop et al, MRM 40:49-54 (1998).
- [7] Sharp and King, MRM 63:151-161 (2010).

Characterizing White Matter in Rat Spinal Cord with Quantitative MRI
Piotr Kozłowski
UBC MRI Research Centre, Vancouver, BC, Canada
<p>Introduction</p> <p>The most significant effect of Spinal Cord Injury (SCI) is the loss of function resulting from white matter damage. Most of the therapeutic procedures in SCI are oriented towards protection and regeneration of the interrupted nerve fiber tracks. Effective testing of these procedures using animal models requires non-invasive technology that can assess changes in white matter over time following a therapy within a particular animal. Examples of various MRI techniques applied to characterize white matter in normal and injured rat spinal cord will be presented.</p> <p>Materials and methods</p> <p>Myelin Water Imaging (MWI) technique was used both in vivo and ex vivo to assess myelin content in normal and injured rat spinal cords. Diffusion Tensor Imaging (DTI) was used to assess axonal damage in rat spinal cords following Dorsal Column Transection (DC Tx) model. Both techniques generated parametric maps at 100 microns in plane resolution, which were correlated with histology.</p> <p>Results</p> <p>Longitudinal MWI study demonstrated the feasibility of high resolution myelin imaging in rat spinal cord in vivo over prolonged periods of time with good reproducibility and low inter-subject and temporal variability.</p> <p>The DC Tx study demonstrated that quantitative MRI can accurately characterize WM damage in a traumatic injury in rat spinal cord ex vivo. We were able to generate high quality MWF maps with in plane resolution sufficient enough to allow quantitative analysis of myelin damage in major DC WM tracts. We showed that in a traumatic spinal cord injury Myelin Water Fraction (MWF) is a more sensitive measure of myelin than transverse diffusivity measured with DTI.</p> <p>Compressed SENSING (CS) multi-echo CPMG with group-sparse reconstruction showed promise at increasing acquisition efficiency in MWI. Through exploiting redundancies in k-space by utilizing intra-image and inter-image correlations, MWF maps were reconstructed with high accuracy from significantly fewer k-space samples, thereby decreasing the acquisition time.</p> <p>Discussion</p> <p>Availability of non-invasive imaging in the preclinical setting greatly facilitates the in vivo analysis of the treated spinal cord injury. Techniques discussed here provide important information about changes in myelin content and neuronal morphology in a clinically relevant model of spinal cord injury. Exact estimation of myelin content in the spared tracts in SCI patients can be a very useful diagnostic tool in assessing neurological and functional outcome of the disease. With improved MRI technology, including high field magnets and multiple receive channels, it may be feasible to implement these techniques a clinical MRI scanner.</p>

Progress in Imaging with the RF Phase Gradient: The TRASE Method
Jonathan C. Sharp, Qunli (Charlie) Deng, Vyacheslav Volotovskyy*, Randy Tyson, Donghui Yin*, Richard Bernhardt*, Scott King*, Boguslaw Tomanek.
NRC Institute for Biodiagnostics (West), Calgary Alberta. *NRC Institute for Biodiagnostics, Winnipeg, Manitoba, Canada
<p>Introduction</p> <p>Transmit Array Spatial Encoding (TRASE) is an MRI method without switched B_0-gradients (Sharp JC & King SB, MRM 2010). TRASE uses the existing RF sub-system to perform the localization tasks normally handled by the B_0-gradient system. The technique uses a new</p>

type of gradient – the RF phase gradient. We believe that this is the first time since the inception of clinical MRI in the 1980s that a viable rival high resolution MRI technology has been proposed. A TRASE sequence consists of an echo train in which the k-space coordinate increases down the echo train, as controlled by the sequence of pulses. Custom RF transmitter coils are required to generate the phase gradient fields. A 1D sequence requires alternation between a positive and negative phase gradient along 1 axis. 2D sequences require 3 or 4 phase gradients. Advantages are: simpler equipment; lower costs; silent imaging; no B0-eddy currents.

RF Coils

Much of our recent work on TRASE has been on RF phase gradient coil designs. A knee coil with two directions of RF encoding has been constructed and tested (0.2T). This 2D coil is constructed from two identical 1D coils, oriented at 90 degrees to each other. Each 1D coil itself consists of two parts: a cosine component and a sine component. These two RF fields are combined normal to each other, with their amplitudes having cosine and sine distributions along the phase gradient direction. Two key aims of the coil development are uniformity of $|B_1|$ and achieving short RF pulse length. 2D in vivo projection images will be presented.

Sequences

TRASE sequences move about k-space by point-reflections. The rules governing the construction of these echo train sequences have and the corresponding k-space trajectories will be presented.

Contrast

Experiments demonstrating T1 and T2 contrasts have been performed in 1D and are directly applicable to 2D imaging.

The 3rd Dimension

We are investigating a number of approaches possible for encoding the 3rd dimension without using switched-B0 gradients (TRASE slice selection; TRASE 3D encoding; static B0-gradient).

Conclusions

The TRASE technique has progressed to the stage of providing high resolution 2D in vivo images. Work remains to be done on developing the most practical method(s) of slice-selection and/or 3D encoding. Nevertheless, there is now good evidence that this method will be capable of yielding diagnostically useful images.

MRI with Ultrashort- (and Zero) Echo Time

Franciszek Hennel

Bruker BioSpin MRI, Ettlingen, Germany

The ability of MRI methods to visualize rapidly decaying signal components is characterized by the Echo Time (TE) - a parameter commonly defined as duration between the excitation RF pulse and the time point when the centre of the k-space, i.e. the coherent signal of the entire object is sampled. Classic MRI sequences contain elements which delay the detection window and inevitably prolong TE: lengthy slice-selective RF pulses, “dephasing” and “phase-encoding” gradient pulses or the redundant “left hand side” part of the echo signal. With currently available gradient amplitudes and switching times, echo times of these sequences can not be set much shorter than a millisecond. Their application range is limited to liquid signal sources and relatively homogenous fields: excellent images can be obtained from soft tissues, but bones, tendons (short T2) or lungs (short T2*) appear as black voids. To access these problematic organs and to allow imaging of quadrupolar nuclei, a sequence called UTE (ultra-short TE, 1) has been proposed that samples the k-space radially, without slice selection, and with the signal being detected during the rising ramp of the readout gradient pulse. The central k-space point is sampled with just a few microseconds delay after the hard RF pulse allowing the visualisation of lung parenchyma or cortical bone structure for the first time. However, artefacts appear in the presence of strong field inhomogeneity, e.g., at interfaces of distinct magnetic susceptibility regions, due to the very low initial amplitude of the encoding gradient.

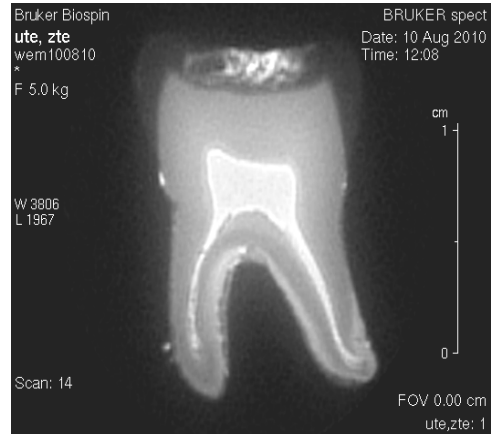


Image of an extracted human tooth obtained with hard-pulse Zero-TE MRI at 11.7 T

An alternative approach consists of exciting the spins and detecting the FID signal in the presence of a constant readout gradient (2). This minimizes the influence of local field offsets and further reduces the duration of acquisition window, which is half gradient ramp shorter than in UTE. The central k-space point is simultaneous with the RF excitation, and is accessible only indirectly; however, according to the common definition, the echo time of the sequence is zero. Zero-TE methods require RF pulses of very high bandwidth, which can be achieved either with short (hard) amplitude-modulated pulses, or with long, frequency sweep pulses. The latter version, proposed with the SWIFT technique (3) requires sampling of the signal in short gaps during application of the pulse. Various recently investigated aspects of hard- and sweep-pulsed Zero-TE imaging (4,5), including the signal-to-noise efficiency and T2 sensitivity will be presented, along with application examples on Bruker animal- and micro-MRI systems.

1. Glover GH et al., *J Magn Reson Imaging*, 2, 47 (1992)
2. Hafner S. et al., *Magn. Reson. Med.*, **181**, 1047 (1994).
3. Idyatullin D. et al., *J. Magn. Reson.*, 342 (2996)
4. M. Weiger, F. Hennel, KP.Pruessmann, *Magn Reson. Med.* **64** 1685-95 (2010)
5. M. Weiger, KP. Pruessmann, F. Hennel, *Magn Reson. Med.* **66** 379-89 (2011)

Real-time Magnetic Resonance Imaging at High Temporal Resolution
Martin Uecker
Biomedizinische NMR Forschungs GmbH, am Max-Planck-Institut für biophysikalische Chemie, Göttingen, Germany
Real-time magnetic resonance imaging (MRI) covers a broad spectrum of applications ranging from studies of turbulent flow to the noninvasive monitoring of interventional procedures. The most important application is cardiac MRI, where real-time MRI may be performed during free breathing and without synchronization to an electrocardiogram. Other applications deal with functional studies of joint movements (temporomandibular joint, knee) or the dynamics of the lips, tongue, and soft palate during speaking or swallowing.

Recently, we described a method for real-time MRI that yields high image quality in terms of temporal fidelity, spatial resolution, signal-to-noise ratio and absence of artifact for frame rates up to 50 Hz. The approach relies on two previously developed methods: It combines strongly undersampled data acquisition using a radially encoded fast low-angle shot (FLASH) sequence with iterative image reconstruction by regularized nonlinear inversion. The latter algorithm was developed for parallel imaging, where the information from multiple receive coils is exploited to reconstruct images from undersampled data. The nonlinear reconstruction algorithm provides a better estimation of the required coil sensitivities than conventional (linear) approaches, which in turn improves the quality of the reconstructed image. Originally formulated for Cartesian sampling, the algorithm can also be used with arbitrary non-Cartesian trajectories, in particular, radial trajectories. This combination of nonlinear inverse image reconstruction with radially encoded data acquisition has many advantageous properties for real-time imaging: It allows for continuous imaging, is highly robust to motion and undersampling, and automatically adapts to changing coil sensitivities for a moving object. Further improvements for dynamic imaging, which exploit the temporal redundancy in a time series of images, enhance the temporal fidelity and quality of the reconstructions.

In the first part of this talk the acquisition technique and the underlying mathematical ideas of the image reconstruction algorithm will be discussed. In the second part, the performance of the method will be demonstrated with various experimental examples.

RF Coils for Microimaging

Krzysztof Jasiński¹, Bogusław Tomaneek^{1,2}, Władysław Węglarz¹

¹Department of Magnetic Resonance Imaging, Institute of Nuclear Physics PAN, ul. Radzikowskiego 152, 31-342 Krakow, Poland, ² Institute for Biodiagnostics, National Research Council of Canada, 435 Ellice Avenue, Winnipeg, Manitoba R3B 1Y6, Canada

Introduction

Microimaging is a rapidly growing field of Magnetic Resonance. Definition of μ MR has evolved in recent years and now it focuses on in vitro studies of volume and mass-limited samples. To facilitate imaging and metabolomics studies at a single cell or cell cluster level, high spatial resolution of several micrometres is needed so dedicated hardware and methods are requisite. In this presentation we will focus on design and optimization of RF coils that provide sufficient SNR necessary for such research.

Subjects and Methods

The size of an RF coil should be matched to the size of the sample to ensure high SNR, so microimaging of small samples makes it necessary to use size-matched RF coils. Imaging of objects smaller than 500 μ m implies fabrication of sub-millimetre sized RF micro-coils. There are two major types of RF micro-coil geometries. Surface coils are usually planar spiral shape while volume coils have well known solenoidal shape. Production of such coils with diameter less than 1mm is difficult without dedicated micro instrumentation. Planar coils are usually produced with application of UV-lithography, etching and electro-deposition, while solenoids could be made of manually wound wire on suitable capillary. As prototype fabrication is time consuming and expensive, we used virtual prototyping by means on 3D FEM simulation to speed up design process. We simulated magneto-static and time harmonic properties of surface and volume microcoils to ensure optimum performance with respect to B_0 and B_1 field homogeneity and high SNR as well. The simulations were carried out with Comsol Multiphysics RF and AC/DC software packages running on 8 core AMD Opteron server equipped with 64GB RAM.

Results

In case of a microcoil, B_0 field deviation induced by differences in the magnetic susceptibility of materials (SU-8 photoresist, Pyrex glass, copper, gold, silicon) used for coil construction is of critical importance, as it introduces difficult to compensate artifacts to MR data. Magnetostatic simulation (AC/DC package) helped to assess impact of material susceptibility variation on B_0 field homogeneity and keep the deviation to absolute minimum. 400MHz harmonic simulation (RF package) enabled coil geometry optimization to obtain desired

region with high B_1 field homogeneity.

This kind of analysis was performed for planar square coils on silicone substrate, gold solenoids wound on SU-8 photoresist molds and a double microstrip coil on PCB. Optimization of double microstrip coil led to conclusion that optimum coil performance is obtained for coils with width (W) to height (H) ratio (W/H) close to 1.

Conclusion

FEM simulation is a valuable tool for RF microcoil design and optimization. Simulation results compare well with measured data [1, 2, 3]. Mass production of inexpensive coils with reproducible characteristics is possible by use of commercially available technology like wire bonding [1] or CMOS IC fabrication process [2].

References

[1] V. Badilita et al. Lab on Chip, 10, 1387, (2010)

[2] J. Anders et al. J. Magn. Reson. 209 (2011) 1–9

[3] K. Jasiński et al. "A Volume Microstrip RF Coil for MRI Microscopy", accepted for publication in: Magnetic Resonance Imaging, Manuscript Number: MRI-D-11-00031R1.

Abstracts of Posters

Bi-modal Molecular Imaging of the Central Nervous System Neoplasm

B.Blasiak^{1,2,3}, T.Foniok³, D.Rushforth³, A.Abulrob^{4,5}, U.Iqbal^{4,5}, H.Albanghdadi^{4,5}, D.Stanimirovic^{4,5}, D.Ponjevic⁶, J.Matyas⁶, T.Veres⁷, G.Sutherland¹, B.Tomanek^{1,2,3}

¹Experimental Imaging Centre, Department of Clinical Neurosciences, University of Calgary, Alberta, Canada,

²Institute of Nuclear Physics, Polish Academy of Sciences, Krakow, Poland,

³Institute for Biodiagnostics (West), National Research Council of Canada, Calgary, Alberta, Canada,

⁴Institute of Biological Sciences, National Research Council Canada, Ottawa, Ontario, Canada,

⁵Faculty of Medicine, University of Ottawa, Ontario, Canada,

⁶Department of Cell Biology and Anatomy, University of Calgary, Alberta, Canada,

⁷Industrial Materials Institute, National Research Council Canada, Boucherville, Quebec, Canada

Brain tumors are one of the most devastating cancers. Despite considerable efforts mean survival for gliomas remains less than one year. Till now MRI has been used for glioma diagnosis with a disputable outcome. Therefore application of molecular sensing would ensure earlier and more accurate diagnosis. An ideal MRI contrast agent is delivered only to a specific cell and provides strong changes in T_2 relaxation times, making the targeted cells detectable with MRI even in small concentrations. The contrast agent used in our molecular MRI comprises Fe_3O_4 core superparamagnetic nanoparticle. The shell, made of dextran, was modified to render such contrast agent multi-modal (MR and IR).

Several different core diameters of Fe_3O_4 (1nm to 40nm) were studied to find the optimum nanoparticle size and concentration. The T_2 relaxation times of agar solutions of the contrast agent were measured using 9.4T MRI system.

A high grade glioma specific sdAb were conjugated with the nanoparticle and IR markers (Cy 5.5.) using amine-functionalized PEG coating, to make contrast agent glioma specific. For in vivo MRI study we used the intracranial injection of U87MG deltaEGFR cells to nude mice, as a model of human high grade glioma. The IR and T_2 -weighted MR images were collected before and after the injection of the contrast agent. A 9.4T MRI system was used to measure T_2 values of the tumor. Using IR and MRI we have shown the efficacy of the new contrast agents, thus potential suitability for the early detection of gliomas.

Acknowledgement: The study was supported by the CIHR Team Grant and EuroCanMRI.

A Feasibility Study of the Severity of Liver Injury in Murine Model of Hepatitis using Gd-EOB-DTPA-enhanced MRI and Texture Analysis

Katarzyna Byk¹, Konrad Jabłoński^{1,2}, Wojciech Szczepański², Paweł Pędrak³, Bogusław Tomanek^{1,4}, Tomasz Skórka¹

¹Polish Academy of Sciences, Institute of Nuclear Physics, Krakow, Poland

²Jagiellonian University Medical College, Krakow, Poland

³AGH University of Science and Technology, Faculty of Physics and Computer Science, Krakow, Poland

⁴National Research Council, Institute for Biodiagnostics, Calgary, Canada

Background: Liver biopsy is a standard approach of liver disease diagnosis. However contrast enhanced MRI as well as quantitative image analysis may be used to provide additional data to that obtained from liver biopsy.

Purpose: To assess liver injury in murine model of Concanavaline A induced hepatitis using contrast-enhanced MR imaging and texture analysis of MR images were performed.

Material and methods: Experiments were performed with a 4.7T/310 magnet (Bruker, Germany), MARAN DRX console (Resonance Instruments, UK) with home-built: gradient coils and RF birdcage coil. Axial MR images were collected using T_1 -weighted gradient echo pulse sequence. 20 BALB/c mice (10 weeks, mean weight 20 g) were divided into four groups based on the Concanavaline (drug inducing the liver disease) administration and accumulated dose: I – control, II – 10 mg/kg ConA, III – 20 mg/kg ConA, and IV – two doses of 10 mg/kg ConA. The last dose of ConA causing acute hepatitis was administered 24 hours before the measurements. Contrast agent Gd-EOB-DTPA (Primovist, Bayer-Shering,

Germany; 0.1 mmol/kg) was injected into the tail vein just after the scout image collection. A time course of pixels intensities of the liver during contrast passage was assessed and texture properties were evaluated using ImageJ (National Institute of Health, USA) software. Texture analysis was performed based on brightness of pixels and co-occurrence matrices. Selected parameters (such as kurtosis, angular second moment, inverse difference moment, entropy) were calculated and compared. Histopathological samples were stained with hematoxylin-eosin and studied under light microscope.

Results: MR images showed the lesions in the liver parenchyma as reticulations dependent on the hepatitis stage severity. Contrast media absorption and removal in the liver was faster in healthy tissue. The measured intensities were higher in groups with zero or insignificant injury (I, II) than in those with considerable tissue injury (III, IV). Histograms mean values shifting and widths changes were caused by distinctions in the image structure that were noticed during contrast metabolism. Time dependencies of the texture features calculated for each group showed different courses. Histopathology showed percentage of hepatocytes necrosis among groups: <5%, 10-25%, >50% (II, III and IV, respectively).

Conclusions: Gd-EOB-DTBA-enhanced MR imaging may be used for acute hepatitis study. Hepatotropic contrast media is absorbed faster by the intact liver, providing higher signal and more homogenous image in the control group as compared to the injured tissue in the ConA treated groups. Quantitative analysis using the texture parameters allowed for the differentiation between groups of animals at different stages of the hepatitis induced liver injury, but it was not sufficient for the individual cases classification.

This work was supported by the European Regional Development Fund from European Union (grant coordinated by JCET-UJ, No WND-POIG.01.01.02-00-069/09-00).

Piecewise Linear Regression and Akaike Information Criterion for the Estimation of the Cardiac Function in Mice

Magdalena Jablonska^{1,2}, Urszula Tyrankiewicz¹, Henryk Figiel², Tomasz Skorka¹

¹H. Niewodniczanski Institute of Nuclear Physics PAS, Department of Magnetic Resonance Imaging, Krakow, Poland

²AGH-University of Science and Technology, Faculty of Physics and Applied Computer Science, Department of Medical Physics and Biophysics, Krakow, Poland

Introduction: Cardiac MRI Time-Volume or single-slice Time-Area Curves (TVC/TAC) illustrate a hemodynamic, multiphase process that describe cardiac function [1]. Character and number of observed TAC phases depends on several factors related to heart and experimental conditions. The aim of this work was to assess Piecewise Linear Regression (PLR) as a tool for the TVC/TAC shape analysis leading to the curve sectioning with estimation of the segments lengths and subsequent smoothing with the use of B-splines.

Subjects and methods: TAC was based on the CMR images acquired in the short axis plane at the papillary muscles level of the mouse LV (cine-like FLASH @ 4.7 T) for arteriosclerosis mouse model (ApoE/LDLR^{-/-}) and the control group at rest and after β -adrenergic stimulation with two dobutamine doses [4]. TAC was modeled with PLR – time was partitioned into intervals and a separate lines were fitted to the each. Position of segments boundaries (breakpoints) were then optimized. The dedicated algorithm was implemented in Matlab software and breakpoints were optimized with Levenberg-Marquard method. Models with different numbers of segments (typically from 3 to 8) were fitted to data and the optimal was selected according to Akaike Information Criterion (AIC) [3].

Results: The proposed multi-linear technique was applied to experimental data. TAC standard parameters like FAC, ER, FR, and IVRT duration were assessed manually by expert and independently by the second operator with the use of PLR. Results obtained from both methods applied at rest and under dobutamine induced stress reveal strong correlation and uncover early stage of cardiac dysfunction in atherosclerotic mice when compared to the control group.

Discussion: PLR was validated as the useful method for tracing qualitative and quantitative changes in TAC shape at rest and after dobutamine stimulation from CMR-based LV single slice images. Appropriate PLR model (according to AIC) significantly accelerate analysis time and allow for automatic and unbiased assessment of TAC with consider of individual systolic and diastolic cardiac phases. Additionally, breakpoints can be used for further analysis, as knots in B-spline method of TACs smoothing for systolic and diastolic peak values calculation.

Acknowledgments: This work was supported by European Regional Development Fund from European Union (grant coordinated by JCET-UJ, No WND-POIG.01.01.02-00-069/09-00).

References: 1. Brutsaert (2006) Prog Cardiovasc Dis; 2. Malash et al. (2010) Chem Eng J; 3. Motulsky, Christopoulos: Fitting model to biological data using linear and nonlinear regression, GraphPad Software Inc. 2003; 4. Tyrankiewicz et al. Book of Abstracts, ESC Heart Failure Congress 2011.

Age Related Alternations in Normal Brain: a Diffusion-weighted Magnetic Resonance Imaging Study

Aleksandra Klimas¹, Ewa Kluczevska², Zofia Drzazga¹

¹ Department of Medical Physics, University of Silesia, Katowice, Poland

² Department of Radiology, Medical University of Silesia, Zabrze, Poland

Purpose: DWI technique is a useful and sensitive method in a large number of clinical and experimental applications i.e. detecting ischemic stroke in its early phase, tumors or assessing neurological disorders in different brain structures. Therefore it seems to be important to know the age dependence of ADC in normal brain.

Method: 89 healthy patients divided into 6 age groups (3-9, 10-19, 20-29, 30-39, 40-49, 50-59, 60-69 years), underwent standard head MRI scan protocol on a 1.5-T GE MRI system. The criterion for normal study was the absence of morphological and signal abnormalities in imaging sequences. DWI was performed for each patient using spin echo EPI with diffusion gradient applied in three orthogonal directions with b-value 0 and 1000 s/mm². ADC values were calculated using ImageJ software for 4 bilateral structures: head of caudate nucleus, thalamus, centrum semiovale and cerebellum. Obtained ADC values were statistically analyzed using student's t-test and ANOVA Tukey's HSD. A p<0,05 was considered to be statistically significant.

Results: The average ADC values for all studied regions of interest showed that the thalamus and centrum semiovale were characterized by the highest while the cerebellum by the lowest values. Differences between right and left side of brain in the subjects were found however they were not significant except thalamus. ADC values in all regions were changed by aging. The correlation between ADC values and age demonstrated complex character. Generally, the ADCs for the youngest groups were decreasing with age, then showed some plateaus to slightly increase for oldest groups (above 50 years). The best relationships in the whole age range were obtained using polynomial fit although with relatively small Pearsons coefficients. For bilateral structures such as head of the caudate nucleus, centrum semiovale and cerebellum correlation coefficients were about R=0.3 while for the other structures lower. However, considering different age ranges it was possible to obtain higher coefficients even up to R=0.8 in the youngest and the oldest groups.

Conclusion: ADC values for chosen bilateral brain structures were determined in wide age range. Mean ADCs showed weaker age dependence for adults compared with the youngest and oldest subjects.

Usefulness of Anisotropic diffusion phantom for DTI
A.T. Krzyżak¹, Z. Raszewski², I. Habina¹, W.Węglarz¹, L.R. Jaroszewicz²
¹ IFJ PAN Kraków, ² WAT Warszawa
<p>Introduction In order to accurately calculate the diffusion tensor using DTI, we must precisely define the matrix b, which depends on the parameters characterizing the imaging sequence [1]. To correctly determine the matrix b we need to know exactly all the gradients and their real shapes. An alternative approach is to eliminate or minimize the impact of gradients other than diffusion gradients. However, this is not always feasible.</p> <p>Subject & method We provide a theoretical basis for this method [2], its advantages and limitations as well as potential sample applications using specially constructed phantoms, characterized by well-known anisotropic diffusion tensor distribution.</p> <p>The presented considerations demonstrate the possibility of using standard phantoms, characterized by the diffusion anisotropy, to determine the matrix b for any sequence of DTI. In test MRI experiments using diffusion version of the PGSE sequence, with reasonable accuracy we calculated the full matrix b for selected directions of the diffusion gradient vector.</p> <p>Results An interesting observation is the existence of statistically significant differences between the components of the matrix b, assigned to different regions of the study area.</p> <p>Conclusions The presented phantom can be used to achieve b-matrix for any direction of diffusion gradients and for any DTI sequence. This method should be especially useful for sequences for which the b-matrix calculation is difficult or impossible. Also seems to be valuable for verification of calculated b-matrix and for numerical correction of gradient field inhomogeneity.</p> <p>References 1. Basser PJ et al JMR(1994)103:247-254 2. Krzyzak AT WO/2009/145648</p> <p>Acknowledgments: Ministry of Science and Higher Education of Poland for grant N518413238 & POIG.01.03.01-14-016/08</p>

Numerical Study of the Quality Factor of MRI RF Coils Made of Normal and HTS Materials
Bartosz J Proniewski¹, Henryk Figiel¹
¹ AGH University of Science and Technology, Faculty of Physics and Applied Computer Science, Department of Medical Physics and Dosimetry, al. A. Mickiewicza 30, 30-059 Krakow, Poland
<p>Quality factor Q of the RF receiver coil directly impacts the signal-to-noise ratio (SNR) and therefore influences the imaging quality of an MRI system. Quality factor is inversely proportional to the equivalent resistance of a receiver RF coil, therefore lowering the resistance should relate to an increased Q. This is especially relevant to low field MRI, where RF coil losses contribute to the majority of noise. In this case of noise predominance, the SNR can be improved by using better conducting materials or lower coil temperatures. Typically RF coils are made of normal conductors therefore cooling down the coil in liquid nitrogen (77 K) results in an increase of the Q factor. An RF receiver coil made of high temperature superconducting (HTS) material should allow for further increase of the Q factor.</p> <p>In this study we adopted the high frequency electromagnetic simulation software (CST Microwave Studio 2011) to model numerically single turn circular surface coils made of HTS, copper and silver conductors. Each coil (10 cm diameter, made of 4.4x0.2 mm conducting tape) was tuned to the resonance frequency at 0.2 T magnetic field, by attaching capacitors</p>

parallel to the coil winding. Model setup consisted of the RF receiver coil and two smaller coils responsible for signal excitation and detection. The simulation employed high-frequency tetrahedral mesh with over 250,000 elements. The CST MWS frequency domain solver was used to simulate the broadband frequency response of the RF coils. Scattering coefficient S_{21} was used to determine the quality factor of the receiver coils under room temperature and cryogenic conditions (liquid nitrogen).

Simulation results showed that building the RF coil using silver material yields an increase of the quality factor of about 2.5%, compared with typically used copper. As both these materials exhibit linear dependence of resistance versus temperature, RF coils operating in liquid nitrogen presented higher values of Q, compared with room temperature results (182 % for silver and 208 % for copper). Receiver coil made of HTS material indicated superior performance out of all simulated scenarios with over fivefold increase of the quality factor, when compared with room temperature results for either copper or silver RF coils.

Performed numerical simulations indicate that quality factor improvement is possible using cryogenic and especially superconducting RF coils. This should directly relate to SNR enhancement for images acquired on a Cirrus Open 0.2 T low field MRI system (MRI-Tech, Poland). Experimental verification on the bench and using phantom images are further planned.

Antyoxidative Properties of Blood Serum: Magnetic Resonance Relaxation Approach

Lech W. Skorski, B. Blicharska

Institute of Physics, Jagiellonian University, Krakow, Poland

A number of biological processes produce the reactive oxygen species (ROS). Cytotoxic action of ROS includes protein, lipid and DNA structure damage and can be primer to many human diseases. In this communication we present the results of our investigation whether the NMR relaxation methods may be used to observe kinetics of oxidative processes in blood serum.

Hydrogen peroxide action is carried out by oxygen, which, from the NMR point of view, is paramagnetic and has an influence on relaxation time. Dependences on time behavior of changes of relaxation times after addition H_2O_2 to serum probe in relation 1:1:8, on various factors like: concentration of Cu and Fe ions in blood serum, presence of antioxidants like Vitamin C or Glutation can give some information about nature and kinetics of these reactions. Proton NMR measurements of relaxation times were performed using a 60 MHz Minispect Bruker spectrometer. Spin-lattice relaxation time T_1 was measured by the Inversion Recovery (IR) sequence, spin-spin T_2 by CPMG method, and the relaxation time in the rotating frame $T_{1\rho}$ was measured using spin-lock pulse sequence ($\pi/2$ - π -spin-lock-FID).

As an introduction the measurements of relaxation times in aqueous hydrogen peroxide solutions as a function of H_2O_2 concentration and temperature were done. It is interesting that in aqueous H_2O_2 solutions T_2 and $T_{1\rho}$ behavior is similar to that obtained for paramagnetic ions like Fe(II) and Cu(II), while for T_1 is almost independent of H_2O_2 concentration up to very high values. When H_2O_2 is added to blood serum, which naturally containing Fe and Cu ions and antioxidants, relaxation times start to change. At the beginning relaxation time T_1 decreases rapidly and, after reaching minimum, start to re-grow. We have observed this behavior only in blood serum.

The measurements of relaxation time are helpful in evaluation of role of antioxidants like Vit.C and Glutation. Antioxidants concentration dependence of relaxation behavior show that presence of these media in solution restrain progress of oxidation. Our results indicate that measurements of relaxation times may be used for the studies of oxidative processes in biological liquids and, in the future, be helpful in investigation of some human diseases background.

A Coupled Spin System Simulator for Pulse Sequence Development and in-vivo Spectrum Quantitation in jMRUI

Zenon Starcuk, Jana Starcukova

Institute of Scientific Instruments, Academy of Sciences of the Czech Republic, Brno, CZ

Introduction: Animal as well as human MR scanners operating at 3 T and above give the access to in vivo MR spectra of metabolites characterized by coupled spin systems. Their spectral multiplets are affected by the volume selective excitation carried out with limited RF power and field gradients, coherence transfer pathway selection, and also by relaxation. The new simulator (NMRScope-B), implemented as a part of jMRUI, has been designed as an easy-to-use tool for both the generation of basis spectra for spectroscopic quantitation and for the study of excitation and quantitation possibilities.

Methods: The simulation of coupled homo- as well as heteronuclear spin systems undergoing relaxation, cross-relaxation and/or magnetization transfer, exposed to spatially and/or frequency-selective excitation, potentially involving phase cycles and/or RF and gradient modulation, is based on density matrix calculations with the Redfield model of relaxation. This core computation takes place in a compiled Matlab kernel, serviced by a java-based GUI that provides access to spin system parameters, simple as well as sophisticated pulse sequence programming, and arraying possibilities suitable for the study of various dependences (spatial selectivity, B₁ sensitivity, offset dependences etc.) on spin system as well as excitation parameters. Arbitrary observable can be examined in an arbitrary set of observation points.

Results: The simulator runs on a range of PCs – netbooks to workstations. The calculation time depends heavily on the computer, the pulse sequence, spin system, and cycling requirements; 7-11 coupled spins seem to be the current practical limit. Simple tasks (individual spectra, excitation profiles, B₁ dependences etc., 7 spins) can be determined mostly in 0.5-5 min, but 20 h may be needed for a glycerophosphorylcholine spectrum.

Conclusions: NMRScopeB provides the ability to simulate coupled and relaxing spin systems undergoing evolutions typical for current MR spectroscopic and spectroscopic imaging sequences. It is suitable for spectroscopic pulse sequence design and the preparation of basis sets for spectroscopic quantitation. The merger of imaging and spectroscopic approaches may be found useful for NMR education. This simulator is available with the latest versions of jMRUI, currently for Windows only.

Acknowledgements: The work was supported by the ASCR grant AV0 Z20650511, GACR grant GA102/09/1861, EC and MEYS CR project No. CZ.1.05/2.1.00/01.0017 and EU Marie Curie Research Network 'FAST', MRTNCT-2006-035801.

In vivo MRI of myocardial infarction induced by hypoxic hypoxia in a murine model (ApoE LDLR^{-/-})

M. Suchanek^{1,2}, U. Tyrankiewicz¹, T. Skórka¹, S. Chłopicki³

¹Institute of Nuclear Physics, Polish Academy of Sciences, ul. Radzikowskiego 152, 31-342 Kraków, Poland

²Department of Chemistry and Physics, Agricultural University, Al. Mickiewicza 21, 31-120 Kraków, Poland

³Department of Pharmacological Analysis, Chair of Pharmacology, Jagiellonian University Collegium Medicum, Grzegorzewska 16, 31-531 Krakow, Poland

Myocardial infarction remains the most common cause of death in the world and is strongly related to coronary atherosclerosis. To increase our knowledge and to evaluate new therapeutic strategies preventing these pathologies a suitable animal model of cardiovascular disease should be developed. The Magnetic Resonance Imaging (MRI) is the method which gives detailed insights into the structure and function of the heart with high temporal resolution allowing for *in vivo* assessment of the cardiovascular system. The aim of this study was to investigate the MRI model of myocardial infarction induced by hypoxia stress.

Ten ApoE LDLR^{-/-} male mice at the age of 7 months were investigated using 4.7 TMRI system. The anesthetized mice (isoflurane, 2%) were first exposed to a pharmacological

stress induced by the dobutamine (2.5 µg/g body weight) and then to hypoxic stress by reducing the oxygen supply. The concentration of oxygen was modified starting at 40% and reducing it down to 5%. After 1.5 min of hypoxic hypoxia the starting O₂ level was restored. The ECG was recorded continuously during the examination using bipolar limb leads in the animal. The MRI was performed using an ECG triggered fast gradient echo (cine-like flow compensated FLASH) sequence. Three cine image series were recorded during the hypoxic hypoxia. For the assessment of the left ventricle (LV) dynamics, nine images per cardiac cycle were acquired in the midventricular short-axis projection at the level of papillary muscles. The time-volume curve was obtained from each series of images by the Aphelion (ADCIS, France/USA) script, providing the following parameters that describe the LV function: stroke area change (SAC), fractional area change (FAC), ejection (ER) and filling (FR) rates.

Our preliminary results demonstrate that the *in vivo* MRI potentially can be a suitable experimental method for the early diagnosis of myocardial infarction that is developed in the mice during hypoxic hypoxia. However, the applied protocol was not sensitive enough to show any clear evidence of the heart disease. For all mice, the only indication of the heart injury was a small decrease (about 10%) of the cardiac output (CO=SAC*HeartRate) product. It could be a consequence of the dobutamine injection. Changing the MRI protocol from 2D imaging to 1D real time imaging could eliminate this artefact.

Acknowledgments: This work was supported by European Regional Development Fund from European Union (grant coordinated by JCET-UJ, No WND-POIG.01.01.02-00-069/09-00).

Image Quality Improvement for the Purpose of the Magnetic Resonance Imaging by the Method of Digital Curvelet Transform

Joanna Świebocka-Więk, Henryk Figiel,

AGH-University of Science and Technology, Faculty of Physics and Applied Computer Science, Al. Mickiewicza 30, 30-059 Cracow, Poland, <mailto:joannasw@agh.edu.pl>

As it is common known, it is highly important to ensure the best diagnostic utilities of the received MRI medical images. Unfortunately it is impossible to avoid some of the disturbances during the acquisition time. Image quality can be described for example by: image contrast, spatial resolution, signal to noise ratio (SNR), the number of artifacts and spatial distortions. Limited frequency spectrum of the received information strongly affects image resolution. In consequence blur of the sharp edges may occur. It may cause the disappearance of small but diagnostically important details of the objects and also anatomical structures. Another problem is noise presence in MRI images which decrease image contrast and small objects visibility as well. Its biggest influence shows up in low contrast parts of the image, close to the visibility threshold. Noise is might be produce by for example magnetic field inhomogeneity, type of coil, the RF pulse, equipment, physical conditions or even acquisition terms. Big number of these parameters causes it is not possible to completely remove the noise from the image; although it is possible to significantly reduce it by the proper image filtration.

In this paper we present a new image quality improvement method - Digital Curvelet Transform (DCT) [1]. It has not been yet tested in the MRI field. This method was proposed by E.J.Candes and D.L.Donoho in 2002 (2nd generation DCT version) [2]. DCT algorithm is a composition of the Discrete Wavelet Transformation (DWT) and the Ridgelet Transformation (RT) what allows more precise edges detection. Application of this method in other scientific fields effects in great results [3] thus we may predict it is going to be very useful in MRI as well.

The algorithm was applied in MATLAB environment basing on the CURVELAB package and tested on phantom and medical images. Main purpose of this presentation is to submit and evaluate the results of the DCT method in MRI based on chosen image quality criteria.

The received result proves high usefulness of DCT for image improvement in the MRI. After DCT filtering, noise is greatly reduced, edges are kept without blurring with high space resolution. DCT algorithm needs for computational time are significantly lower in comparison

to other filtering methods. Nevertheless the method complexity is still high due to application of additional transformation procedure (RT). DCT application additionally gives possibility of 3D signal processing which could be very useful in MRI.

Main conclusion of our research is that the DCT algorithm can be applied to improve MRI images with very good results and its further development is strongly recommended.

References:

- [1] D.L. Donoho and M.R. Duncan, *Digital Curvelet Transform: Strategy, Implementation and Experiments*; Technical Report, Stanford University 1999
- [2] E.J. Candès and D.L. Donoho *New Tight Frames of Curvelets and Optimal Representation of Objects with Smooth Singularities*, <http://www.curvelet.org>, 2002
- [3] J.L. Starck., E.J. Candès and D.L. Donoho., *The Curvelet Transform for Image Denoising*, IEEE Trans. on Image Processing, Vol. 11, Issue 6

Biphasic Stress-test Protocol in R of Diastolic Properties of the Mouse Models of Heart Failure

Urszula Tyrankiewicz¹, Tomasz Skorka¹, Magdalena Jablonska^{1,2}, Katarzyna Byk¹, Stefan Chlopicki³

¹ Institute of Nuclear Physics, Polish Academy of Sciences, Department of Magnetic Resonance Imaging, Krakow, Poland

² AGH University of Science and Technology, Department of Medical Physics and Biophysics, Krakow, Poland

³ Jagiellonian University Medical College, Department of Experimental Pharmacology, Krakow, Poland

Purpose: Cardiac stress examination is valuable method that allows describing cardiac function in different stage of impairment. The goal of this study was to assess the cardiac function and reserve using low and high dobutamine stimulation in order to analyze the level of diastolic impairment in three murine models of cardiovascular pathology: (1) Tgαq*44, that develop dilated cardiomyopathy (2) doxorubicin induced heart failure and (3) ApoELDLR-/- model that develop sever atherosclerosis at the age of 6 months with and without LCHP diet.

Methods and Materials: Tgαq*44 mice (at the late stage of HF), ApoELDLR/- (at the advanced stage of atherosclerosis) and doxorubicin treated mice (for 5 weeks/twice weekly/2mg/kg, i.p.; two weeks after the last injection) were used with their strain matched controls groups. Left ventricle (LV) function was assessed using 4.7T/310 magnet (Bruker) system with MARAN DRX console (Resonance Instruments) at baseline and after low and high (0.5 and 5 mg/kg, i.p.) dobutamine stimulation based on: End Systolic/ Diastolic Area (ESA/EDA), Ejection/ Filling Rate (ER/FR), Heart Rate (HR), Fractional Area Change (FAC), Slice Cardiac Output (SCO).

Results: We observed: (1) decreased in ER, FR, FAC with increased in ESA at rest condition and biphasic response to dobutamine in Tgαq*44 mice (enhanced cardiac reserve for low dose in FR, ER and ESA and enhanced HR with fall in EDA for peak stimulation); (2) decrease in EDA and SCO parameter at rest and after low and high dobutamine stimulation with no FR changes in doxorubicin treated animals; (3) decrease at rest and after dobutamine stimulation in FR and normal EDA values as compared to the control, with increased ER, ESA and wall thickness in atherosclerotic mice.

Conclusion: Low and high dobutamine stimulation was beneficial in examination of specific diastolic properties in different mouse HF models and with the use of MRI allow to uncovered: (1) biphasic "hypoxia-like" response that may suggest the secondary endothelial impairment of coronary vessels in Tgαq*44 mice (2) development of HF as decreased SCO in doxorubicin model (3) isolated diastolic impairment in atherosclerotic mice when treated with diet. In conclusion, MR imaging protocol with two levels of stimulation may facilitate research investigation by uncovering additional characteristics of murine heart failure pathologies.

This work was supported by European Regional Development Fund from European Union

Methods of Myocardial Strain Measurement in Tagged Magnetic Resonance Imaging

Konrad Werys^{1,2}, Joanna Petryka¹, Łukasz Błaszczuk^{1,2}, Kamil Szwaba^{1,2}, Ewa Piątkowska-Janko², Błażej Sawionek², Piotr Bogorodzki², Jolanta Miśko¹

¹ Cardiovascular Magnetic Resonance Group, Institute of Cardiology, Warsaw, Poland

² Institute of Radioelectronics, Warsaw University of Technology, Poland

Cardiovascular diseases are one of a major cause of morbidity and mortality in the Western World. Among many non-invasive methods of heart disease diagnosis, tagged magnetic resonance imaging is the best fitted to observe myocardium kinematics.

Many algorithms were developed in order to obtain the quantitative information about the motion of the heart from tagged magnetic resonance images. This study focuses on the myocardial strain, which is a motion parameter with proved diagnostic value, especially in the myocardial dyssynchrony disease.

Many methods used in strain calculation are based on tracking the motion of myocardium elements. This approach faces problems connected with the spatial nature of the heart movement, which can be observed on planar images. In this study we compare three methods based on a different approach: the Harmonic Phase, its modification with the use of the Gabor filter bank and a method based on image processing with the use of Gabor filters. All of these methods allow for a calculation of strain without the use of motion tracking.

Harmonic Phase (HARP) algorithms enable calculation of motion parameters directly from the tagged images. It turns out that each of these spectral peaks carry information about a particular component of tissue motion. To extract this information, the Fourier transform of each peak is performed in order to obtain a harmonic phase image. Motion parameters are calculated directly from the harmonic phase image.

The main problem of the HARP method is a correct isolation of the spectral peak. A possible modification is the use of the Gabor filter bank. The advantage of this method over other types of filtering is a better selectivity in frequency and spatial domain. The difference is clearly visible in the case of big deformations.

Another approach is a method fully based on the Gabor filters. It combines a local fitting of the Gabor filter with the use of optimization algorithms. Once the parameters of the best fitted filter are known, it is possible to calculate the distance between the tagging lines. Once this is done, the other motion parameters may be computed.

The aim of this study was to compare the three described methods. First, a software model of the heart was built with a given set of motion parameters. Then, the motion parameters of the model were compared with results generated through the use of the three processing methods. This allowed for a calculation of errors in the strain estimation.

The error off the method fully based on the Gabor filters was smaller than in the case of the other two methods. This is especially visible in the case of big deformations. The main disadvantage of this method, however, is a significantly higher time necessary for obtaining the calculation.

The Potential Applications of Dispersion Profiles Method in NMR Scans Contrast

¹Dorota Wierzuchowska, ²Barbara Blicharska, ²Lech W. Skórski,

¹Institute of Physics, Pedagogical University, Podchorążych 2, 30-084 Kraków, Poland

²Institute of Physics, Jagiellonian University, Reymonta 4, 30-059 Kraków, Poland

The investigation of NMR relaxation properties of biological systems *in vitro* provide a powerful tools for *in vivo* tissue anatomy and function imaging. One of NMR methods in research on the properties of macromolecules systems is a "dispersion profile", which is a

dependence of spin-lattice relaxation time $T_{1\rho}$ in rotating frame plotted as a function of low magnetic field B_1 . This method gives an unique opportunity to observe the slow molecular motion in the range typical for water associated with proteins and bio-molecules.

Our researches are focused on the connections of obtained parameters of molecular dynamics with the conformation changes of protein samples. NMR relaxation studies were performed using Bruker Minispec NMR spectrometer working at a proton resonance frequency 60 MHz. We report the results of $T_{1\rho}$ dispersion profiles measurements for samples of egg white and bovine serum albumins and lysozyme – lyophilized powders and its aqueous solutions under different conditions. The obtained dispersion profiles were analyzed using two potential relaxation models: dipole–dipole interaction and power law. Although both of them satisfactorily describe dispersion of magnetic relaxation and can be used to estimate molecular dynamic parameters but dipolar model allows to evaluate the correlation times in the simplest way and is more clear by results interpretation. Obtained parameters are strongly associated with the changes of protein system structure.

Image contrast in clinical MRI determined by the $T_{1\rho}$ difference of water proton relaxation provide novel information about molecular dynamics in tissues (for example: in the case of brain ischemia *in vivo*). Presented $T_{1\rho}$ dispersion profile method of investigation is easier and faster than previous approaches involving measurements of the temperature and field dependences of spin-lattice relaxation times. For this reasons we hope that the current results *in vitro* give a new information on protein systems and can be helpful in contrast study of tissue imaging *in vivo*.

Attendees List

Dr. Abedelnasser Abulrob
Cerebrovascular Research Group
Institute for Biological Sciences
National Research Council

Dr. Tomasz Banasik
MRI
Institute of Nuclear Physics
Polish Academy of Sciences

Dr. Barbara Blasiak
Clinical Neurosciences
Faculty of Medicine
University of Calgary

Mr. Łukasz Błaszczak
Instytut Kardiologii im. Prymasa
Tysiąclecia Stefana Kardynała
Wyszyńskiego

Prof. dr hab. Barbara Blicharska
Radiospectroscopy
Institute of Physics
Jagiellonian University

Ms. Katarzyna Byk
MRI
Institute of Nuclear Physics
Polish Academy of Sciences

Prof. dr hab. Marian Cholewa
Physics
Rzeszow University of Technology

Dr. Roxanne Deslauriers
Institute for Biodiagnostics
National Research Council

Prof. Henryk Figiel
Medical Physics and Dosimetry
Faculty of Physics and Applied
Computer Science
AGH University of Science and
Technology

Dr. Jens-Christoph Georgi
Healthcare Sector, Imaging &
Therapy division
Magnetic Resonance, H IM MR MK O
Siemens AG

Prof. dr. hab. Pawel Grieb
Mossakowski Medical Research
Centre

Dr. Sylwia Heinze-Paluchowska
MRI
Institute of Nuclear Physics
Polish Academy of Sciences

Dr. Franciszek Hennel
Bruker Medical

Dr. Uwe Himmelreich
Biomedical NMR Unit/MoSAIC
Katholieke Universteit Leuven

Dr. Jan-Bernd Hövener
Medical Physics
Department of Diagnostic
Radiology
University Hospital Freiburg

Ms. Magdalena Jabłońska
MRI
Institute of Nuclear Physics
Polish Academy of Sciences

Prof. Karol Jackowski
Department of Chemistry
Warsaw University

Mr. Krzysztof Jasiński
MRI
Institute of Nuclear Physics
Polish Academy of Sciences

Dr. Scott King
MR Technology
Institute for Biodiagnostics
National Research Council

Ms. Aleksandra Klimas
Medical Physics
Institute of Physics
University of Silesia

Dr. Piotr Kozłowski
The Prostate Centre in Vancouver

Dr. Artur Krzyzak
MRI
Institute of Nuclear Physics
Polish Academy of Sciences

Dr. Piotr Kulinowski
MRI
Institute of Nuclear Physics
Polish Academy of Sciences

Dr. Stanisław Kwieciński
MRI
Institute of Nuclear Physics
Polish Academy of Sciences

Mr. Radoslaw Leszczynski
Bruker Polska

Dr. Andrew Lonergan
MRI Sales and Business
Development, Scandinavia,
Netherlands, UK, and Poland
Bruker UK Limited

Dr. Luca Menichetti
Cardiovascular Magnetic
Resonance Laboratory
CNR Istituto di Fisiologia Clinica

Dr. Aygul Mert
Neurosurgery
Medical University Vienna

Dr. Harald Möeller
Max Planck Institute for Human
Cognitive and Brain Sciences
Max Planck Institute for Human
Cognitive and Brain Sciences

Dr. Daniel Muruve
Faculty of Medicine
University of Calgary
Dr. Andre Obenaus
Non-Invasive Imaging Laboratory
Loma Linda University
Chan Shun Pavilion, Room A1010

Dr. Mihaela Onu
Department of Radiology
Prof. Dr. T. Burghele Hospital

Ms. Anna Osiak
MRI
Institute of Nuclear Physics
Polish Academy of Sciences

Artur Ostrowski
Siemens Healthcare

Dr. Tadeusz Palasz
Institute of Physics
Jagellonian University

Mr. Bartosz Proniewski
Medical Physics and Dosimetry
Faculty of Physics and Applied
Computer Science
AGH University of Science and
Technology

Michal Pytel
Siemens Healthcare

Dr. Franz Schmitt
Coordination 7T
Siemens AG, MED MREF

Dr. Jonathan Sharp
MR Technology
Institute for Biodiagnostics (West)
National Research Council

Dr. Tomasz Skórka
MRI
Institute of Nuclear Physics
Polish Academy of Sciences

Mr. Lech Skorski
Radiospectroscopy
Institute of Physics
Jagiellonian University

Dr. Ian Smith
Institute for Biodiagnostics
National Research Council

Dr. Ray Somorjai
Biomedical Informatics
Institute for Biodiagnostics
National Research Council

Dr. Danica Stanimirovic
Neurobiology Program
Institute for Biological Sciences
National Research Council

Dr. Zenon Starcuk
Ústav prístrojové techniky

Dr. Mateusz Suchanek
MRI
Institute of Nuclear Physics
Polish Academy of Sciences

Ms. Joanna Świebocka-Więk
Medical Physics and Biophysics
Physics and Applied Computer
Science Department
AGH University of Science and
Technology

Krzysztof Szybinski
Siemens Healthcare

Dr. Ganghong Tian
Cardiac Studies
Institute for Biodiagnostics
National Research Council

Dr. Boguslaw Tomanek
MR Technology
Institute for Biodiagnostics
National Research Council

Dr. Krzysztof Turek
Medical Physics and Biophysics
Physics and applied computer
Science
AGH University of Science and
Technology

Ms. Urszula Tyrankiewicz
MRI
Institute of Nuclear Physics
Polish Academy of Sciences

Dr. Martin Uecker
Biomedizinische NMR Forschungs
GmbH
am Max-Planck-Institut für
biophysikalische Chemie

Dr. Władysław Węglarz
MRI
Institute of Nuclear Physics
Polish Academy of Sciences

Mr. Konrad Werys
Instytut Kardiologii im. Prymasa
Tysiąclecia Stefana Kardynała
Wyszyńskiego

Dr. Dorota Wierzuchowska
Institute of Physics
Pedagogical University

Uniz.Doż. Stefan Wolfsberger
Medizinische Universität Wien
Universitätsklinik für
Neurochirurgie
Allgemeines Krankenhaus der Stadt
Wien - Universitätskliniken

Mr. Grzegorz Woźniak
MRI
Institute of Nuclear Physics
Polish Academy of Sciences

Conference Maps

A) Hotel and Conference Location

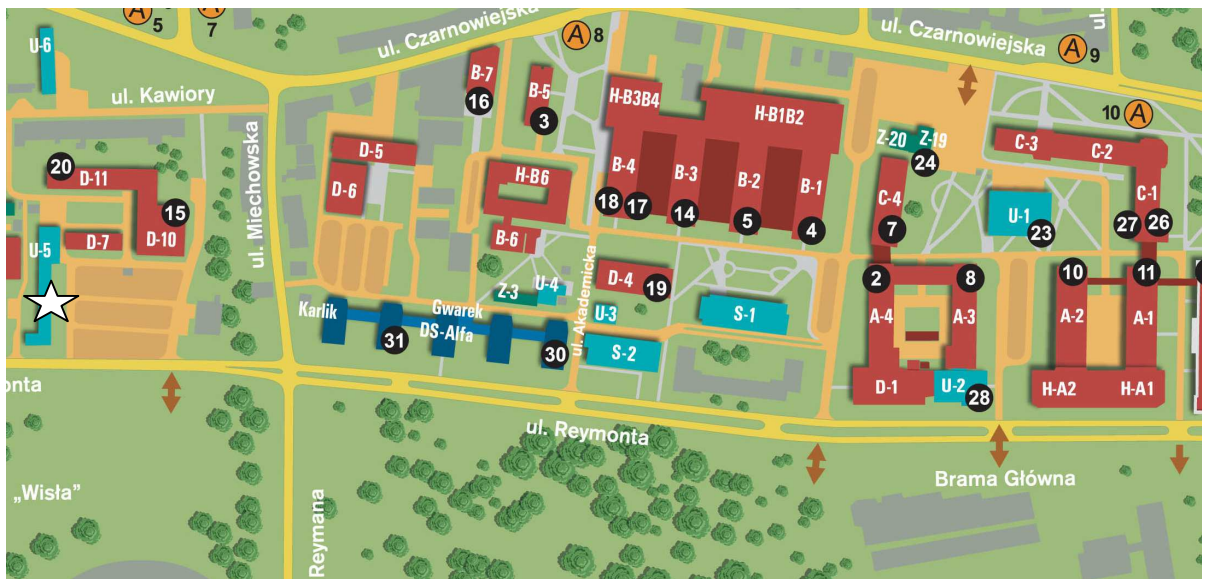


☆ Conference location, AGH University of Science and Technology, 30 Mickiewicza Ave., Building C1, second floor, room 224

◇ Polonez Hotel, 15 Reymonta Street

Map courtesy of AGH University of Science and Technology

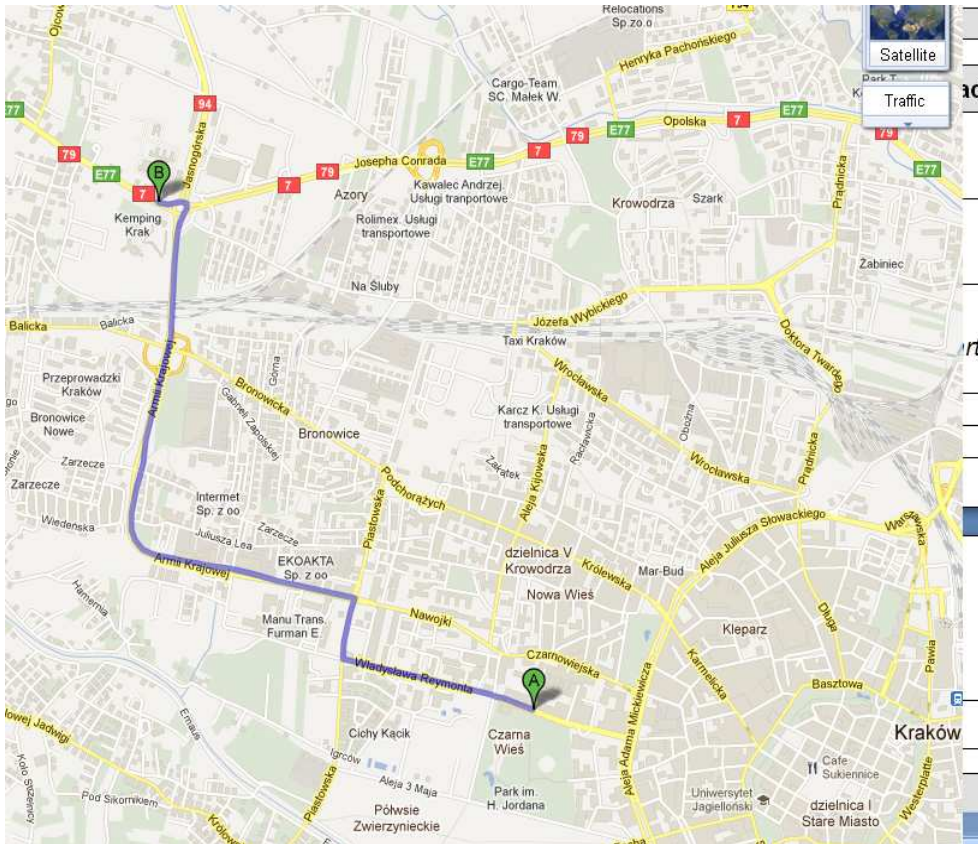
B) 0.2T location



☆ 0.2T is located in building U5, AGH University of Science and Technology

Map courtesy of AGH University of Science and Technology

C) 9.4T Institute for Nuclear Physics



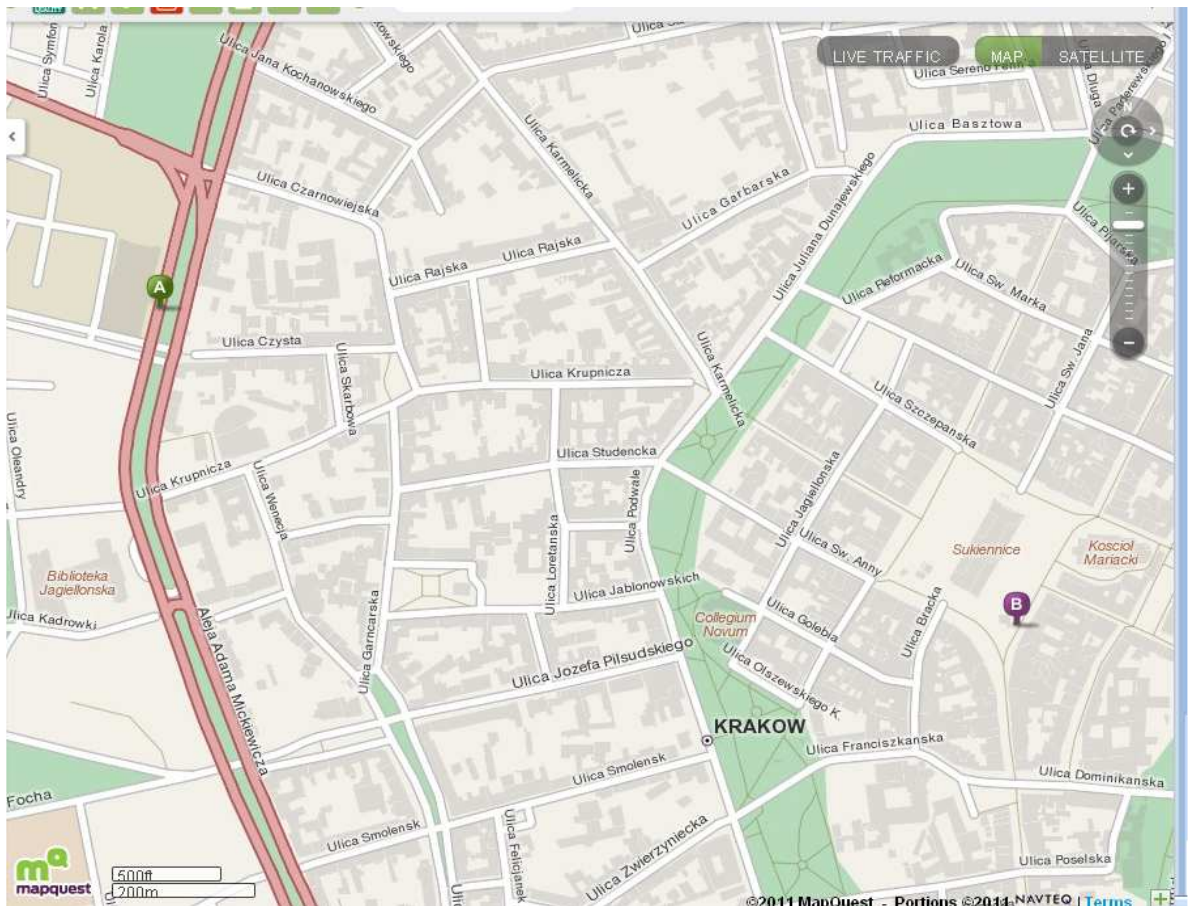
A) Polonez Hotel, 15 Reymonta Street

B) H. Niewodniczanski Institute of Nuclear Physics, Ul. Radzikowskiego 152

*Transportation by bus from/to Polonez hotel will be provided

Map created from Google maps

D) Map from AGH University of Science and Technology to the Main Square



A) AGH University of Science and Technology, 30 Mickiewicz Ave.

B) Sukiennice, Rynek Główny (Cloth Hall, Main Square)

Maps via Maquest